

# Carbonate saturation state of surface waters in the Ross Sea and Southern Ocean: controls and implications for the onset of aragonite undersaturation

H. B. DeJong<sup>1</sup>, R. B. Dunbar<sup>1</sup>, D. Mucciarone<sup>1</sup>, D. A. Koweeck<sup>1</sup>

[1]{Department of Earth System Science, Stanford University, Stanford, CA, USA }

Correspondence to: H. B. DeJong ([hdejong@stanford.edu](mailto:hdejong@stanford.edu))

## Abstract

Predicting when surface waters of the Ross Sea and Southern Ocean will become undersaturated with respect to biogenic carbonate minerals is challenging in part due to the lack of baseline high resolution carbon system data. Here we present ~ 1700 surface total alkalinity measurements from the Ross Sea and along a transect between the Ross Sea and southern Chile from the austral autumn (Feb-Mar 2013). We calculate the saturation state of aragonite ( $\Omega_{Ar}$ ) and calcite ( $\Omega_{Ca}$ ) using measured total alkalinity and  $pCO_2$ . In the Ross Sea and south of the Polar Front, variability in carbonate saturation state ( $\Omega$ ) is mainly driven by algal photosynthesis. Freshwater dilution and calcification have minimal influence on  $\Omega$  variability. We estimate an early spring surface water  $\Omega_{Ar}$  value of ~1.2 for the Ross Sea using a total alkalinity-salinity relationship and historical  $pCO_2$  measurements. Our results suggest that the Ross Sea is not likely to become undersaturated with respect to aragonite until the year 2070.

## 1 Introduction

Atmospheric  $CO_2$  concentrations have increased by 40% since preindustrial times to ~400 ppm today and could reach 936 ppm by the year 2100 (IPCC AR5 WG1, 2013). Due to oceanic uptake of  $CO_2$ , surface ocean pH is already 0.1 units lower than preindustrial values and is projected to decrease by another 0.3-0.4 units by the end of the century, equivalent to a 50% decrease in carbonate ion ( $CO_3^{2-}$ ) concentrations (Orr et al., 2005). Even after  $CO_2$  emissions are

1 halted, it will take thousands of years before the surface ocean pH returns to preindustrial levels  
2 (Caldeira and Wickett, 2003; Archer et al., 2009).

3 The saturation state ( $\Omega$ ) of seawater with respect to a specific calcium carbonate ( $\text{CaCO}_3$ )  
4 mineral (aragonite, calcite, or magnesium calcite) is defined as:

$$5 \quad \Omega = \frac{[\text{Ca}^{2+}][\text{CO}_3^{2-}]}{K_{sp}} \quad (1)$$

6 where  $K_{sp}$  is the solubility product constant for the specific  $\text{CaCO}_3$  mineral and depends on  
7 salinity, temperature, and pressure (Mucci, 1983). Aragonite is ~ 1.6 times more soluble than  
8 calcite at 0°C whereas the solubility of magnesium calcite varies depending on the mole fraction  
9 of magnesium ions (Dickson, 2010).  $\Omega_{Ar}$  represents the saturation state of aragonite and  $\Omega_{Ca}$   
10 represents the saturation state of calcite.  $\Omega < 1$  represents undersaturation where dissolution is  
11 thermodynamically favorable and  $\Omega > 1$  represents supersaturation where precipitation is  
12 favorable. Most surface waters of the global oceans are currently supersaturated with respect to  
13  $\text{CaCO}_3$  (Feely et al., 2009). However, for some species including coccolithophorids,  
14 foraminifera, and tropical corals, decreasing  $\text{CO}_3^{2-}$  concentrations can decrease calcification rates  
15 even in supersaturated conditions (Riebesell et al., 2000; Moy et al., 2009; Andersson et al.,  
16 2011).

17 The Southern Ocean is especially vulnerable to Ocean Acidification (OA) due to its relatively  
18 low total alkalinity (TA) and because of increased  $\text{CO}_2$  solubility in cold water. In addition,  
19 Antarctic continental shelves have insignificant sedimentary  $\text{CaCO}_3$  to buffer against OA (Hauck  
20 et al., 2013). Modeling studies predict that surface waters in the Southern Ocean may start to  
21 become undersaturated with respect to aragonite by 2050 and be fully undersaturated by 2100  
22 (Orr et al., 2005; Feely et al., 2009). McNeil and Matear (2008) have suggested that wintertime  
23 aragonite undersaturation in the Southern Ocean may begin as early as 2030.

24 OA induced decreases in  $\Omega$  have potentially serious consequences for Antarctic food webs. In  
25 the Ross Sea the aragonitic shelled pteropod *Limacina helicina* is a dominant zooplankton that  
26 can reach densities of 300 individuals  $\text{m}^{-3}$  (Hopkins, 1987; Seibel and Dierssen, 2003; Hunt et  
27 al., 2008). Pteropods are important prey for nototheniid fish, which in turn are major prey for  
28 penguins, seals, and whales (Foster and Montgomery, 1992; La Mesa et al., 2000; 2004).  
29 Pteropods may also be important contributors to the biological pump (Collier et al., 2000;

1 Accornero et al, 2003; Manno et al., 2010). Orr et al. (2005) found that the shell of a subarctic  
2 pteropod started to dissolve within 48 h when placed in waters with the level of aragonite  
3 saturation expected to occur in the Southern Ocean by 2100. Severe dissolution pitting was  
4 observed on live pteropods that were collected from the upper 200 meters in the Atlantic sector  
5 of the Southern Ocean, from waters that were near undersaturation with respect to aragonite  
6 (Bednaršek et al., 2012).

7 Other organisms in the Southern Ocean may be negatively impacted by OA include krill  
8 (Kawaguchi et al., 2013), foraminifera (Moy et al., 2009), sea urchins (Sewell and Hofmann,  
9 2011), deep sea hydrocorals (Shadwick et al., 2014), seastars (Gonzalez-Bernat et al., 2013),  
10 bivalves (Cummings et al., 2011), and brittle stars (McClintock et al., 2011). Conversely non-  
11 calcareous phytoplankton may benefit in the Ross Sea in a high pCO<sub>2</sub> world, especially the larger  
12 diatom *Chaetoceros lineola* (Tortell et al., 2008; Feng et al., 2009).

13 There are only a few surface carbon system data sets from the Ross Sea (Bates et al, 1998;  
14 Sweeney et al., 2000b; Sandrini et al., 2007; Long et al., 2011; Mattsdotter Björk et al., 2014;  
15 Rivaro et al., 2014; Kapsenberg et al., 2015) that can be used to establish baselines in order to  
16 understand the relative importance of physical, chemical, and biological processes that drive the  
17 large spatial and seasonal variability of  $\Omega$ . With no winter  $\Omega$  measurements, it is challenging to  
18 predict when the Ross Sea will become undersaturated with respect to aragonite and calcite. A  
19 model by McNeil et al. (2010) suggests that winter surface waters in the Ross Sea will become  
20 undersaturated with respect to aragonite by the year 2045 since sea ice, upwelling of deep water,  
21 and short residence times prevent these surface waters from reaching equilibrium with the  
22 atmosphere. However, McNeil et al. (2010) indirectly estimated surface winter  $\Omega_{Ar}$  values by  
23 using limited carbon system data from the spring (Sweeney et al., 2000b).

24 We present ~1700 underway TA measurements from the surface waters of the Ross Sea and  
25 along a transect across the Southern Ocean from the Ross Sea to southern Chile. By combining  
26 the underway TA measurements with pCO<sub>2</sub> data we characterize the complete carbon system and  
27 describe patterns and controls on  $\Omega$  variability. Finally, after establishing a relationship between  
28 salinity and TA, we use the Lamont Doherty Earth Observatory (LDEO) pCO<sub>2</sub> database  
29 (Takahashi et al., 2009) (available at <http://www.ldeo.columbia.edu/res/pi/CO2>) to provide an  
30 independent estimate of Ross Sea surface water  $\Omega_{Ar}$  in early spring.

## 1    **2        Study site**

2    The Antarctic Circumpolar Current (ACC) flows from east to west around the entire Antarctic  
3    continent and is composed of multiple fronts that separate distinct water masses (Rintoul et al.,  
4    2001). There are three primary fronts—the southern ACC front (SACCF), the Antarctic Polar  
5    Front (PF) and the Subantarctic Front (SAF) (Orsi et al., 1995). Sokolov and Rintoul (2009)  
6    found that these primary fronts are composed of multiple jets that they label south (S), middle  
7    (M), and north (N). Convergent Ekman transport north of the westerly wind stress maximum  
8    (near the axis of the ACC) downwells surface water into the ocean interior. Circumpolar Deep  
9    Water (CDW) upwells south of the wind stress maximum where it becomes modified into  
10    Antarctic surface water (AASW) (Rintoul et al., 2001).

11    The cyclonic Ross Sea gyre is located south of the ACC (Smith et al., 2012). The southern  
12    portion of this gyre flows west along the Ross Sea continental slope and generates intrusions of  
13    CDW onto the Ross Shelf through the major troughs (Orsi et al., 2009; Dinniman et al., 2011;  
14    Kohut et al., 2013). In addition, AASW enters the Ross Sea in the east and flows westward along  
15    the Ross Ice Shelf (Orsi et al., 2009).

16    The Ross Sea is considered a biological hotspot supporting over 400 benthic species (Smith et  
17    al., 2012). During the winter the Ross Sea is mostly covered by sea ice, which begins to clear in  
18    November to form the largest polynya in Antarctica. There are two main phytoplankton blooms  
19    in the Ross Sea. The first bloom begins in late November in the Ross Sea polynya (Fig. 1a) and  
20    peaks in mid to late December (Arrigo et al., 1999, 2004). In early January, sea ice melts in the  
21    western Ross Sea lowering surface salinity and increasing stratification (Fig. 1b). As a result, a  
22    secondary diatom bloom forms in the west with productivity peaking in late January to early  
23    February (Arrigo et al., 1999, 2004) (Fig. 1c).

24    The Ross Sea phytoplankton blooms account for up to half of all primary production over the  
25    Antarctic continental shelf (Arrigo and McClain, 1994; Smith and Gordon, 1997; Arrigo and van  
26    Dijken, 2003). Photosynthesis reduces the concentration of nutrients and dissolved inorganic  
27    carbon (DIC) in the mixed layer, causing  $\Omega$  to increase in surface waters (McNeil et al., 2010).  
28    Once the sea ice reforms during autumn and winter, remineralization of organic matter and deep  
29    convective mixing produces a relatively homogeneous water column, causing surface DIC

1 concentrations to increase and  $\Omega$  to decrease (Gordon et al., 2000; Sweeney et al., 2000b; Petty  
2 et al., 2013).

3

## 4 **3 Methods**

### 5 **3.1 Analytical methods**

6 As part of the TRacing the fate of Algal Carbon Export (TRACERS) program, we undertook  
7 continuous measurements of surface water TA in the western Ross Sea aboard the *Nathaniel B*  
8 *Palmer* (NBP13-02) from 13 Feb through 9 March 2013. In addition, from 19 Mar to 2 Apr  
9 2013, we made continuous measurements of surface water TA in transit between the Ross Sea  
10 and southern Chile along the cruise track shown in Fig. 2. Underway TA measurements were  
11 conducted using the shipboard uncontaminated continuous flow system with an intake located at  
12 ~ 5 m depth. Seawater from the ship's underway system was redirected to the bottom of a 250  
13 mL free surface interface cup flowing at 2 L/min and was drawn from the bottom of the cup for  
14 TA analysis without filtration. The entire system was automated and relatively unattended. The  
15 sampling cycle was every 24 minutes on a custom-configured Metrohm 905 Titrand equipped  
16 with three Metrohm 800 Dosino syringe pumps (two 50 mL units for sample handling and  
17 rinsing and one 5 mL unit for acid titration). Temperature was measured at the cup and in the  
18 titration cell. We used certified 0.1N HCl provided by A. Dickson (Scripps Institution of  
19 Oceanography) for the potentiometric titrations and TA calculations follow Dickson et al.  
20 (2003). Since we consumed the certified HCl after ~ 1000 measurements in the Ross Sea, we  
21 have no TA data from the eastern Ross Sea. For the transect to southern Chile, we mixed our  
22 own 0.1N HCl solution (from 12.1N HCl, laboratory grade NaCl, and deionized water). We  
23 calibrated TA measurements using certified reference materials (CRMs) Batch 122 provided by  
24 A. Dickson (Scripps Institution of Oceanography). Our estimated precision for the underway TA  
25 measurements from 68 CRM analyses is  $\pm 3 \mu\text{mol kg}^{-1}$  ( $\pm 1$  SD).

26 Outlier TA analyses were identified by taking a running mean and standard deviation of 9  
27 consecutive measurements. A measurement was rejected if (1) the difference between the  
28 measurement and mean was greater than twice the standard deviation and (2) the difference  
29 between the measurement and mean was greater than  $6 \mu\text{mol kg}^{-1}$ . A total of 65 measurements  
30 (out of 1716) were rejected.

1 We collected seawater samples for particulate organic carbon (POC) every 2 h from the ship's  
2 continuous flow system between the Ross Sea and Chile. Following the protocols of Knap et al.  
3 (1996), we filtered 1 to 3 L of seawater through precombusted Whatman GFC filters and  
4 immediately rinsed these filters with 10 mL of 0.01N HCl to remove carbonate. We air dried the  
5 filters before sending them to Stanford University where they were analyzed on a Carlo Erba  
6 NA1500 Series 2 elemental analyzer.

7 Surface pCO<sub>2</sub> measurements were made every 3 minutes using the LDEO air-sea equilibrator  
8 permanently installed on the NBP (data available at <http://www.ldeo.columbia.edu/res/pi/CO2>).  
9 The estimated precision is  $\pm 1.5 \mu\text{atm}$ .

10 Underway salinity and sea surface temperature (SST) were measured continuously by the ship's  
11 thermosalinograph (TSG) (Sea-Bird Model SBE-45). These variables were binned into 1 minute  
12 intervals.

13 We collected discrete water samples at 85 stations in the Ross Sea from 13 Feb through 18 Mar  
14 2013 (Fig. 1a). We used a rosette sampler fitted with 24 Niskin bottles and a Sea-Bird Model  
15 SBE-911+ conductivity, temperature, and depth (CTD) sensor. We also measured salinity on  
16 discrete underway and hydrocast samples at 25°C using a Guildline 8400 Autosal four-electrode  
17 salinometer. The difference between the Autosal measurements and salinity from the  
18 conductivity sensor was less than 0.02. In this paper we use the hydrocast samples to evaluate the  
19 controls of seasonal surface  $\Omega_{\text{Ar}}$  variability. The water column data will be further analyzed in  
20 upcoming papers.

21 We collected hydrocast samples for TA and DIC following the protocols of Dickson et al. (2007)  
22 and immediately added saturated mercuric chloride (< 0.1% by volume). For TA, we ran each  
23 sample within 12 h of collection using a second potentiometric titrator, a Metrohm 855 Robotic  
24 Titrosampler equipped with two 800 Metrohm Dosino syringe pumps (one 50 mL unit for rinsing  
25 and sample handling and one 5 mL unit for acid titration). The samples were prefiltered through  
26 0.45 $\mu\text{m}$  polyvinylidene fluoride filters and the estimated precision based on the CRMs (n=108)  
27 is  $\pm 1.5 \mu\text{mol kg}^{-1}$ .

28 We measured DIC on hydrocast samples within ~ 4 h of collection without filtration. We  
29 acidified 1.25 mL of the sample using a custom built injection system coupled to an infrared gas  
30 analyzer (LI-COR LI7000). As described by Long et al. (2011), the infrared absorption signal

1 versus time is integrated for each stripped gas sample to yield a total mass of CO<sub>2</sub>. Samples were  
2 run in triplicate or greater and were calibrated using CRMs between every 3-4 unknowns. Micro-  
3 bubbles regularly appeared within injected samples due to sample warming between acquisition  
4 and DIC analysis. Each integration curve was visually inspected and integration curves that  
5 exhibited evidence for bubbles were rejected. The estimated precision based upon unknowns  
6 (>3500 runs) and CRM replicates (n=855) for cruise NPB-1302 is  $\pm 3 \mu\text{mol kg}^{-1}$ .

7

### 8 **3.2 Carbon system calculations and crosschecks**

9 We calculate  $\Omega$  and DIC (hereafter called DIC<sub>calc</sub>) for underway samples with CO2SYS for  
10 MATLAB (Lewis and Wallace, 1998; van Heuven et al., 2009) with TA, pCO<sub>2</sub>, SST, and  
11 salinity as input variables. Calculations are only conducted for pCO<sub>2</sub> measured within 3 minutes  
12 of the TA measurement (n=1034), the average cycle time for the automated pCO<sub>2</sub> measurements.  
13 We use the equilibrium constants of Mehrback et al. (1973) as refit by Dickson and Millero  
14 (1987) since previous studies have found that they are the optimal choice, including for Antarctic  
15 waters (Lee et al., 2000; Millero et al., 2002; McNeil et al., 2007). For the hydrocast data, we  
16 calculate  $\Omega$  using TA, DIC, temperature, and salinity as input variables.

17 As a means of internal quality control, we use the initial pH reading from the TA titration as a  
18 third carbon system parameter to crosscheck the accuracy of our  $\Omega_{\text{Ar}}$  estimates.  $\Omega_{\text{Ar}}$  calculated  
19 using TA and pCO<sub>2</sub> is  $0.02 \pm 0.07$  greater than  $\Omega_{\text{Ar}}$  calculated using TA and pH. In addition,  
20 DIC<sub>calc</sub> using TA and pCO<sub>2</sub> is  $2 \pm 7 \mu\text{mol kg}^{-1}$  lower than DIC<sub>calc</sub> using TA and pH. Finally,  
21 measured pCO<sub>2</sub> is  $4 \pm 14 \mu\text{atm}$  lower than pCO<sub>2</sub> calculated from TA and pH. These strong  
22 consistencies suggest that our pCO<sub>2</sub> and TA measurements are accurate. Our surface TA and  
23 DIC<sub>calc</sub> measurements versus latitude for the Southern Ocean are within the ranges of other  
24 studies (, Metzl et al., 2006; McNeil et al., 2007; Mattsdotter Björk et al., 2014).

25 We compare the TA measurements from the surface hydrocasts (< 5 meters deep) to the  
26 underway TA measurements made while the ship was still on station within ~ 15 minutes of  
27 when the surface samples were collected. The underway values are  $3 \pm 5 \mu\text{mol kg}^{-1}$  higher than  
28 the hydrocast TA values.

29

### 1 3.3 Ross Sea and Southern Ocean Calculations

2 The  $\Omega_{Ar}$  of surface waters in the Ross Sea increases during the austral summer months (McNeil  
3 et al., 2010). We use DIC, TA, SST, and salinity to determine the controls on the seasonal cycle  
4 of surface water  $\Omega_{Ar}$ . We normalize DIC and TA to a salinity of 34.5, the average salinity of the  
5 Ross Sea (hereafter called sDIC and sTA). Due to the deep convective mixing during the winter,  
6 we use the average sDIC and sTA concentrations of hydrocast samples collected from 200-400  
7 m to determine winter water values (sDIC =  $2221 \pm 5 \mu\text{mol kg}^{-1}$ , sTA =  $2338 \pm 3 \mu\text{mol kg}^{-1}$ ).  
8 While sDIC and sTA concentrations below 200 m are influenced by carbon export particularly in  
9 the summer and early autumn, observations show that sDIC and sTA concentrations are  
10 relatively uniform below 200 m across space and a given season (Table 1).

11 Following Hauri et al. (2013), the change in  $\Omega_{Ar}$  of surface hydrocast samples (upper 10 m) from  
12 winter conditions can be expressed as:

$$13 \Delta\Omega_{Ar} = \frac{\partial\Omega}{\partial DIC} \Delta sDIC + \frac{\partial\Omega}{\partial TA} \Delta sTA + \frac{\partial\Omega}{\partial T} \Delta T + \Delta S_{\Omega} + Residuals \quad (2)$$

14 where

$$15 \Delta S_{\Omega} = \frac{\partial\Omega}{\partial S} \Delta S + \frac{\partial\Omega}{\partial DIC} \Delta DIC^s + \frac{\partial\Omega}{\partial TA} \Delta TA^s \quad (3)$$

16  $\Delta sDIC$  and  $\Delta sTA$  are the difference in sDIC and sTA for each sample from the winter value. The  
17 term  $\Delta T$  is calculated using a winter SST of  $-1.89^{\circ}\text{C}$  (per Sweeney, 2003).  $\Delta S_{\Omega}$  represents the  
18 total contribution of salinity changes to  $\Delta\Omega_{Ar}$ .

19 Since salinity between 200 to 400 m is variable across the Ross Sea (Orsi and Wiederwohl,  
20 2009),  $\Delta S$  is calculated as the difference between the salinity of a surface sample and the average  
21 salinity for samples from that station that are between 200-400 m.

22  $\Delta DIC^s$  and  $\Delta TA^s$  represent changes to DIC and TA due to dilution/concentration from freshwater  
23 input and sea-ice processes:

$$24 \Delta DIC^s = [DIC_{200-400} * (\text{Salinity}_{\text{surface sample}}/\text{Salinity}_{200-400})] - DIC_{200-400} \quad (4)$$

$$25 \Delta TA^s = [TA_{200-400} * (\text{Salinity}_{\text{surface sample}}/\text{Salinity}_{200-400})] - TA_{200-400} \quad (5)$$

26  $DIC_{200-400}$ ,  $TA_{200-400}$ , and  $\text{Salinity}_{200-400}$  are the average values for samples collected from 200-  
27 400 m calculated at each station.



1 The partial derivatives quantify the change in  $\Omega_{Ar}$  per unit change in DIC, TA, temperature, and  
2 salinity respectively. To determine the partial derivatives, we calculate  $\Omega_{Ar}$  for all hydrocast  
3 samples within the upper 10 m using DIC, TA, temperature, and salinity as input parameters. We  
4 recalculate  $\Omega_{Ar}$  after independently increasing DIC, TA, temperature, and salinity by one unit.  
5 The partial derivatives are the average difference between the initial  $\Omega_{Ar}$  and the recalculated  
6  $\Omega_{Ar}$ .

7 We use the same equations to evaluate the relative importance of DIC, TA, temperature, and  
8 salinity on the variability of  $\Omega_{Ar}$  from 75°S to 55°S. For the  $\Delta$  terms, we calculate the change in  
9 sDIC, sTA, temperature, and salinity from the mean of the first 6 underway measurements at  
10 75°S. For Eq. 4 and Eq. 5, instead of using DIC, TA, and salinity values from 200-400 m, we use  
11 the mean of the first 6 underway measurements at 75°S.

12

## 13 **4 Results and Discussion**

### 14 **4.1 $\Omega$ in the Ross Sea**

15 Underway TA values range from 2268 to 2346  $\mu\text{mol kg}^{-1}$  (mean =  $2314 \pm 16 \mu\text{mol kg}^{-1}$ ). Since  
16 TA strongly covaries with salinity ( $R^2=0.86$ , residual  $\pm 6 \mu\text{mol kg}^{-1}$ ), the lowest TA values are  
17 located in the west where the salinity is lowest (Fig. 1b). Values of sTA range from 2336 to 2386  
18  $\mu\text{mol kg}^{-1}$  (mean =  $2360 \pm 7 \mu\text{mol kg}^{-1}$ ) and are influenced by calcification/dissolution as well as  
19 phytoplankton photosynthesis since one unit of nitrate drawdown increases TA by one unit  
20 (Brewer and Goldman, 1978) (Fig. 1d).

21 Surface  $\text{pCO}_2$  values range from 162 to 354  $\mu\text{atm}$  and are lower in the west due to late season  
22 phytoplankton photosynthesis (Fig 1e). Surface  $\Omega_{Ar}$  ranges from 1.40 to 2.42 and  $\Omega_{Ca}$  ranges  
23 from 2.24 to 3.89 (Fig. 2f). The highest  $\Omega_{Ar}$  values are also located in the west. Phytoplankton  
24 photosynthesis increases  $\Omega$  by both decreasing DIC and increasing TA.

25 Spatial and temporal variations in surface water  $\Omega_{Ar}$  are mainly controlled by sDIC in the Ross  
26 Sea (Eq. 2, Fig. 3). The concentration of sDIC decreased by  $58 \pm 20 \mu\text{mol kg}^{-1}$  from a winter  
27 value, causing  $\Omega_{Ar}$  to increase by  $0.5 \pm 0.2$ . In addition, sTA increased by  $11 \pm 7 \mu\text{mol kg}^{-1}$   
28 during the preceding summer months, causing  $\Omega_{Ar}$  to increase by  $0.1 \pm 0.1$ . Although there was a  
29 significant reduction in salinity compared to winter values ( $0.7 \pm 0.3$ ),  $\Omega_{Ar}$  only decreased by ~

1 0.01 due to this freshening since both DIC and TA concentrations were reduced. Lastly, the  
2 effect of temperature on  $\Omega_{Ar}$  was negligible since the Ross Sea only experiences a 2°C seasonal  
3 change in SSTs (Sweeney, 2003).

4 Two processes can reduce sDIC, calcification and phytoplankton photosynthesis. To evaluate the  
5 importance of calcification, we use time dependent changes in potential alkalinity (PALK =  
6 sNitrate + sTA) from a winter value ( $2367 \pm 3 \mu\text{mol kg}^{-1}$ , defined as average value for all  
7 samples between 200-400 m). While TA will increase during photosynthesis due to nitrate  
8 drawdown, PALK will be conserved. Therefore, changes in PALK can be attributed to  
9 calcification and dissolution. The average  $\Delta\text{PALK}$  from a winter concentration is negligible ( $0 \pm$   
10  $5 \mu\text{mol kg}^{-1}$ ); therefore, calcification appears to be insignificant and the increase in sTA from  
11 winter conditions is largely driven by nitrate drawdown during photosynthesis. Earlier studies  
12 found that calcification contributed to only ~ 5% of the total seasonal DIC drawdown (Bates et  
13 al., 1998; Sweeney et al., 2000a). Therefore, we argue that photosynthesis exerts the dominant  
14 control on sDIC, sTA, and  $\Omega_{Ar}$ . While the highest  $\Omega_{Ar}$  value that we observed was 2.4, values up  
15 to ~ 4 have been observed during Dec-Jan (McNeil et al., 2010). By the time we arrived in the  
16 Ross Sea, surface sDIC concentrations would have already increased relative to the summer due  
17 to enhanced air-sea  $\text{CO}_2$  fluxes (Arrigo and Van Dijken, 2007), deepening of the mixed layer  
18 (Sweeney, 2003), and remineralization of organic carbon (Sweeney et al., 2000b).

19 Mattsdotter Björk et al. (2014) also argue that phytoplankton photosynthesis is the major control  
20 on surface water  $\Omega_{Ar}$  variability between the Ross Sea and the Antarctic Peninsula based upon  
21 the covariance of  $\Omega_{Ar}$  and chlorophyll-a. The largest contributor to seasonal  $\Omega_{Ar}$  change in the  
22 Chukchi Sea in the Arctic is also phytoplankton photosynthesis (Bates et al., 2013). However,  
23 unlike the Ross Sea, numerous studies have also demonstrated aragonite undersaturation of  
24 surface waters in parts of the Arctic due to sea ice melt and river runoff (Chierici and Fransson,  
25 2009; Yamamoto et al., 2009; Robbins et al., 2013).

26

## 27 **4.2 $\Omega$ in the Southern Ocean**

28 The spatial changes in  $\Omega_{Ar}$ , SST,  $\text{pCO}_2$ , and POC between 75°S and 55°S are shown in Fig. 4.  
29 We also include the mean location of the fronts from Sokolov and Rintoul (2009) as they  
30 intersect our cruise track. The lowest  $\Omega_{Ar}$  value is 1.25 ( $\Omega_{Ca} = 2.00$ ) at 75°S, corresponding with

1 the highest  $p\text{CO}_2$  of  $\sim 396 \mu\text{atm}$ .  $\Omega_{\text{Ar}}$  increases along the transect to reach a maximum of 1.93  
2 ( $\Omega_{\text{Ca}} = 3.04$ ) at  $55^\circ\text{S}$ . The changes in  $\Omega_{\text{Ar}}$  are not always monotonic. In two regions changes in  $\Omega_{\text{Ar}}$   
3 can be attributed to enhanced primary production. Between  $74^\circ\text{S}$  and  $73^\circ\text{S}$ ,  $\Omega_{\text{Ar}}$  first increases  
4 and then decreases by  $\sim 0.1$ . This corresponds with a  $40 \mu\text{atm}$  drop and then rise in  $p\text{CO}_2$ . Given  
5 that SST is constant, this localized increase in  $\Omega_{\text{Ar}}$  is likely due to phytoplankton photosynthesis.  
6 This region may be along the Antarctic Slope Front that is known for higher biological activity  
7 (Jacobs, 1991). There is another step in  $\Omega_{\text{Ar}}$  from  $\sim 1.4$  to  $\sim 1.55$  between  $68^\circ\text{S}$  and  $66^\circ\text{S}$  across the  
8 SACCF-N. This step also corresponds with a decrease in  $p\text{CO}_2$  from  $\sim 370$  to  $\sim 340 \mu\text{atm}$ .  
9 Elevated POC concentrations between the SACCF-N and the PF-M correspond with these lower  
10  $p\text{CO}_2$  values and again indicate enhanced phytoplankton photosynthesis. Ruben (2003) also  
11 found that  $p\text{CO}_2$  is reduced south of the PF ( $170^\circ\text{W}$ ) due to primary production.

12 To further gain insight into why  $\Omega_{\text{Ar}}$  increases along our transect, we quantify the contribution of  
13 changing  $s\text{DIC}$  (calculated from TA and  $p\text{CO}_2$ ),  $s\text{TA}$ , SST, and salinity to changing  $\Omega_{\text{Ar}}$  (Fig.  
14 5a). The dominant control is declining  $s\text{DIC}_{\text{calc}}$  from  $\sim 2240$  to  $\sim 2140 \mu\text{mol kg}^{-1}$  between  $75^\circ\text{S}$   
15 and  $55^\circ\text{S}$ , which causes  $\Omega_{\text{Ar}}$  to increase by 0.87 if  $s\text{TA}$ , SST, and salinity are held constant (Fig.  
16 6). Declining  $s\text{TA}$  from  $\sim 2340$  to  $\sim 2310 \mu\text{mol kg}^{-1}$  partially counters the influence of  $s\text{DIC}_{\text{calc}}$   
17 and reduces  $\Omega_{\text{Ar}}$  by 0.28. The influences of SST and salinity on  $\Omega_{\text{Ar}}$  are minimal.

18  $\Omega_{\text{Ar}}$  variability is driven almost entirely by changes in  $s\text{DIC}_{\text{calc}}$  from  $75^\circ\text{S}$  to the PF-S. Between  
19 the PF-S and the SAF-N, variability in  $\Omega_{\text{Ar}}$  is influenced by the opposing effects of  $s\text{DIC}_{\text{calc}}$  and  
20  $s\text{TA}$ . The TA: $\text{DIC}_{\text{calc}}$  ratio and  $\Omega_{\text{Ar}}$  are constant between the PF-S and the SAF-S since both  
21  $s\text{DIC}_{\text{calc}}$  and  $s\text{TA}$  decrease at the same rate (Fig. 5b). Between the SAF-S and the SAF-N,  $\Omega_{\text{Ar}}$   
22 increases since  $s\text{DIC}_{\text{calc}}$  declines faster than  $s\text{TA}$ . North of the SAF-N,  $\Omega_{\text{Ar}}$  variability is again  
23 driven by  $s\text{DIC}_{\text{calc}}$ .  $\Omega_{\text{Ar}}$  increases due to a decrease in  $s\text{DIC}_{\text{calc}}$  while  $s\text{TA}$  remains constant.

24 We examine possible controls on  $s\text{DIC}_{\text{calc}}$  along the transect. The concentration of  $s\text{DIC}_{\text{calc}}$  is  
25 highest south of the PF-S due to upwelling of CDW (Fig. 6a). To evaluate the properties of  
26 CDW, we use data from the 2011 Repeat Hydrography Cruise SO4P, which is part of the U.S.  
27 Climate Variability and Predictability (CLIVAR) program (Swift and Orsi, 2012) (available at  
28 <http://www.clivar.org/resources/data/hydrographic>). We only use data from hydrocasts located  
29 between  $168^\circ\text{E} - 73^\circ\text{W}$  where the bottom depth is  $>1000 \text{ m}$  (Fig. 2b). We reject the data from  
30 hydrocast 46(B) where the deep DIC data below 200 m is  $\sim 30 \mu\text{mol kg}^{-1}$  higher than the rest of

1 the stations. Following Sweeney (2003), CDW is defined as centered on the level of maximum  
2 temperature below 150 m.

3 From this CLIVAR dataset, CDW has a sDIC value of  $2243 \pm 3 \mu\text{mol kg}^{-1}$ . Between  $75^\circ\text{S}$  and  
4  $74^\circ\text{S}$ , sDIC<sub>calc</sub> concentration of surface water is also  $2243 \pm 5 \mu\text{mol kg}^{-1}$ , indicating little  
5 modification to CDW and consistent with the observation that this region was covered by sea ice  
6 even during the summer of 2013. At  $74^\circ\text{S}$  sDIC<sub>calc</sub> drops to  $\sim 2220 \mu\text{mol kg}^{-1}$  and by  $66^\circ\text{S}$ , across  
7 the SACCF-N, sDIC<sub>calc</sub> drops to  $\sim 2200 \mu\text{mol kg}^{-1}$ . This  $40 \mu\text{mol kg}^{-1}$  decrease in sDIC<sub>calc</sub>  
8 between Antarctica and the PF-S is consistent with the observed drops in pCO<sub>2</sub> that we attributed  
9 to photosynthesis. Ruben et al. (1998) also observed a 30-50  $\mu\text{mol kg}^{-1}$  decrease in sDIC at  $67^\circ\text{S}$   
10 in Pacific Antarctic waters between winter and summer that they attribute to primary  
11 productivity.

12 sDIC<sub>calc</sub> continues to drop from  $\sim 2220 \mu\text{mol kg}^{-1}$  at the PF-S to  $\sim 2140 \mu\text{mol kg}^{-1}$  at  $55^\circ\text{S}$ ,  
13 consistent with surface DIC measurements between  $70^\circ\text{S}$  and  $40^\circ\text{S}$  compiled by McNeil et al.  
14 (2007). There are multiple factors likely responsible for this decrease in sDIC<sub>calc</sub>. Both satellite  
15 (Arrigo et al., 2008) and in situ measurements (Reuer et al., 2007) show that annual primary  
16 productivity increases from south to north in the Southern Ocean. In addition, surface waters  
17 north of the PF advect northwards and accumulate a sDIC deficit. Finally, warmer water holds  
18 less DIC while in equilibrium with the atmosphere. There is little net air-sea CO<sub>2</sub> flux between  
19  $75^\circ\text{S}$  and  $55^\circ\text{S}$  (except for net efflux at  $60^\circ\text{S}$ ) since warming and increased biological production  
20 compensate each other (Takahashi et al., 2012).

21 We also examine possible controls on sTA concentrations along the transect. The concentration  
22 of sTA is also highest south of the PF-S due to upwelling of CDW. Based off the CLIVAR  
23 dataset, the sTA of CDW is  $2334 \pm 3 \mu\text{mol kg}^{-1}$ . The sTA of surface water between  $74^\circ\text{S}$  and the  
24 PF-S is  $\sim 2340 \mu\text{mol kg}^{-1}$ , slightly higher than its CDW source (Fig. 6b). Nitrate drawdown  
25 during photosynthesis may explain the elevated sTA. Between  $75^\circ\text{S}$  and  $74^\circ\text{S}$ , sTA exceeds  $2360$   
26  $\mu\text{mol kg}^{-1}$ . One possible explanation is that ikaite ( $\text{CaCO}_3 \cdot 6\text{H}_2\text{O}$ ), a mineral that has been  
27 observed directly and indirectly to precipitate in Antarctic sea ice (Dieckmann et al., 2008;  
28 Fransson et al, 2011), dissolved into surface waters during the summer causing sTA  
29 concentrations to increase. Between the PF-S and SAF-N, sTA drops to  $2310 \mu\text{mol kg}^{-1}$  where  
30 the concentrations level off. This drop appears to be in part due to the mixing of two end member

1 water masses, AASW south of the PF-S and Subantarctic surface water north of the SAF-N. The  
2 decreasing sTA is consistent with the suggestion of Millero et al. (1998) that a negative linear  
3 relationship between sTA and SST is due to colder water being indicative of greater upwelling of  
4 TA rich water.

5 This dataset supports the argument that increased upwelling of CDW from strengthening  
6 westerly winds will increase OA in the Southern Ocean (Lenton et al., 2009). While the TA:DIC  
7 ratio for CDW is  $1.040 \pm 0.002$ , the TA:DIC<sub>calc</sub> ratio for surface waters between 75°S and the  
8 PF-S ranges from 1.046 to 1.064 (Fig. 5b). Therefore increased upwelling will lower the TA:DIC  
9 ratio and cause  $\Omega_{Ar}$  to decrease.

10

### 11 **4.3 Estimate of wintertime surface $\Omega_{Ar}$ values in the Ross Sea**

12 Efforts to predict winter  $\Omega_{Ar}$  undersaturation in the Ross Sea are complicated by the complete  
13 lack of carbon system measurements from the winter months in the Ross Sea.

14 McNeil et al. (2010) estimated winter surface water  $\Omega_{Ar}$  by using the lowest observed  $\Omega_{Ar}$  value  
15 from early spring when the Ross Sea is still covered by sea ice. They used mid October and early  
16 November carbon system measurements from the Joint Global Ocean Flux Study (JGOFS)  
17 (Sweeney et al., 2000b). Although sea ice algae productivity peaks in November, their impact on  
18 water column DIC concentrations is likely to be negligible (Saenz and Arrigo, 2014). McNeil et  
19 al. (2010) found that early spring surface water  $\Omega_{Ar}$  was  $\sim 1.2$ . There was a single  $\Omega_{Ar}$  value  $< 1.1$   
20 that they used as an initial condition along with the IPCC US92a scenario to predict that surface  
21 waters of the Ross Sea could begin to experience seasonally undersaturated conditions with  
22 respect to aragonite as early as 2015 if full equilibrium with rising atmospheric CO<sub>2</sub> is achieved.  
23 Based on a three-dimensional Coupled Ice, Atmosphere, and Ocean model (Arrigo et al., 2003,  
24 Tagliabue and Arrigo, 2005), McNeil et al. (2010) argued that only 35% of the atmospheric CO<sub>2</sub>  
25 signal equilibrates with Ross Sea surface waters due to sea ice, upwelling of CDW, and short  
26 residence times, thereby delaying the onset of aragonite undersaturation until 2045. Decadal  
27 wintertime surface carbon system measurements do not exist to directly validate this  
28 disequilibrium assumption. In addition, McNeil et al. (2010) would inaccurately predict when the  
29 Ross Sea would become undersaturated with respect to aragonite if the minimum wintertime  
30 surface  $\Omega_{Ar}$  value used was low due to measurement error.

1 To independently calculate  $\Omega_{Ar}$  from early spring surface waters, we use the LDEO pCO<sub>2</sub>  
2 measurements from November 1994, 1997, 2005, and 2006 that are from the Ross Shelf (defined  
3 by the 1000m isopleth) and are south of 74°S (Fig. 7a). The earliest pCO<sub>2</sub> measurements are  
4 from 16 Nov 1994, 17 Nov 1997, 6 Nov 2005, and 13 Nov 2006 when much of the Ross Sea is  
5 still covered in sea ice. The earliest measurements from 2005/06 are more likely to represent  
6 winter conditions since they are from 74°S as the NBP entered the Ross Sea. Conversely, the  
7 earliest measurements from 1994/97 are from the 76.5°S line, close to where the Ross Sea  
8 polynya opens up from.

9 We calculate wintertime TA in the Ross Sea by establishing a salinity-TA relationship using data  
10 from Bates et al. (1998), Sweeney et al. (2000b), and our own hydrocast TA measurements from  
11 the upper 10 m (Fig. A1). Since one unit of nitrate drawdown increases TA by one unit, the TA  
12 measurements are adjusted to winter nitrate concentrations of 29  $\mu\text{mol kg}^{-1}$  (the mean nitrate  
13 concentration between 200-400 m from our cruise). The relationship between TA and salinity is  
14 consistent among these independent datasets and the standard deviation of the residuals for TA is  
15  $\pm 5 \mu\text{mol kg}^{-1}$ .

16 We calculate historical  $\Omega_{Ar}$  using historical pCO<sub>2</sub> measurements, salinity derived TA, SST, and  
17 salinity. Phosphate and silicate are set to the winter values of 2.1  $\mu\text{mol kg}^{-1}$  and 79  $\mu\text{mol kg}^{-1}$   
18 respectively. The TSG salinity data from the historical pCO<sub>2</sub> measurements appears reasonable  
19 and is uncalibrated. While the largest offset in TSG salinity compared with Autosal  
20 measurements is 0.3, such error is not typical. To test the possible impact of a poor salinity  
21 calibration, we recalculate  $\Omega_{Ar}$  for all pCO<sub>2</sub> measurements after increasing salinity by 0.3. TA  
22 calculated from the observed TA-salinity relationship increases by  $\sim 21 \mu\text{mol kg}^{-1}$  and  $\Omega_{Ar}$   
23 increases by  $0.024 \pm 0.003$ .

24 The lowest  $\Omega_{Ar}$  measurements are 1.24 in 1994, 1.25 in 1997, 1.22 in 2005, and 1.20 in 2006  
25 (Fig. 7b). Although  $\Omega_{Ar}$  declines from 1994 to 2006, we have low confidence in any trend due to  
26 spatial-temporal sampling biases. The lowest  $\Omega_{Ar}$  values are consistently between 1.2 and 1.3 as  
27 the ship crossed sea ice covered regions and open water that had experienced DIC drawdown.  
28 With the exception of a single measurement, the lowest 1996/97  $\Omega_{Ar}$  values from McNeil et al.  
29 (2010) are also  $\sim 1.2$ . The similarity between the  $\Omega_{Ar}$  values reported by McNeil et al. (2010)  
30 from 1996/97 and our 2005/06 values is consistent with their delayed acidification hypothesis.

1 A simple calculation also suggests that wintertime  $\Omega_{Ar}$  values may be closer to 1.2 than 1.1. If  
2 salinity is 34.5, approximately the mean salinity of the water column, TA would be 2339  $\mu\text{mol}$   
3  $\text{kg}^{-1}$  based on the observed TA-salinity linear relationship. Sweeney (2003) estimates winter  
4  $\text{pCO}_2$  values of  $\sim 425 \mu\text{atm}$  based on deep  $\text{pCO}_2$  measurements made during early spring. Setting  
5 salinity to 34.5, TA to 2339  $\mu\text{mol kg}^{-1}$ ,  $\text{pCO}_2$  to 425  $\mu\text{atm}$ , temperature to  $-1.89$ , silicate to 79  
6  $\mu\text{mol kg}^{-1}$ , and phosphate to 2.1  $\mu\text{mol kg}^{-1}$  yields a  $\Omega_{Ar}$  value of 1.22.

7 Although  $\text{pCO}_2$  measurements of surface waters colder than  $-1.75^\circ\text{C}$  south of  $60^\circ\text{S}$  typically  
8 reach  $\sim 410 \mu\text{atm}$  by September, Takahashi et al. (2009) present a few measurements of  $\sim 450$   
9  $\mu\text{atm}$ . Even if  $\text{pCO}_2$  reaches 450  $\mu\text{atm}$  during winter in the Ross Sea,  $\Omega_{Ar}$  would be 1.16 (with  
10 salinity at 34.5 and TA at 2339  $\mu\text{mol kg}^{-1}$ ). In order to obtain  $\Omega_{Ar}$  of 1.1,  $\text{pCO}_2$  would need to be  
11  $\sim 480 \mu\text{atm}$ , a value that appears unreasonably high given the available datasets from the Ross  
12 Sea.

13 McNeil et al. (2010) calculated the  $\Omega_{Ar}$  of water arriving onto the Ross Shelf following the  
14 recipes of Jacobs and Fairbanks (1985): 50% CDW, 25% Tmin water (minimum temperature in  
15 upper 100 m), and 25% AASW. To calculate the  $\Omega_{Ar}$  of these three source water masses, they  
16 used hydrocast temperature, salinity, and DIC data collected during the austral winter of 1994  
17 from north of the Ross Shelf as described in Sweeney (2003). They calculated that the average  
18  $\Omega_{Ar}$  of incoming water would be 1.08.

19 We independently calculate  $\Omega_{Ar}$  of incoming water using the 2011 CLIVAR hydrocast data from  
20 north of the Ross Shelf between  $168^\circ\text{E} - 73^\circ\text{W}$  as described earlier (Fig. 2b). The  $\Omega_{Ar}$  of water in  
21 the upper 100 m (AASW and Tmin) from the CLIVAR dataset is  $1.36 \pm 0.13$  and the  $\Omega_{Ar}$  of  
22 CDW (maximum temperature below 150 m) is  $1.18 \pm 0.03$  (Fig. A2). Even if 100% of the  
23 incoming water onto the Ross Shelf is CDW, the  $\Omega_{Ar}$  of this incoming water would be greater  
24 than 1.08. While most properties of CDW are similar between the 2011 CLIVAR data and the  
25 1994 data used by McNeil et al. (2010), the TA of CDW from the CLIVAR dataset is 18  $\mu\text{mol}$   
26  $\text{kg}^{-1}$  higher (Table 2).

27 Another approach to estimate the  $\Omega_{Ar}$  of winter surface waters is to use the properties of water  
28 below 200 m. For the TRACERS data, sTA below 200 m is  $2338 \pm 2 \mu\text{mol kg}^{-1}$ . For the JGOFS  
29 autumn cruise (NBP 97-3) sTA below 200 m is  $2339 \pm 2 \mu\text{mol kg}^{-1}$ . Using the CLIVAR dataset,

1 sTA of CDW from off the Ross Shelf is  $2334 \pm 3 \mu\text{mol kg}^{-1}$ . This consistency between  
2 independent datasets suggests that we can accurately estimate winter TA in the Ross Sea.

3 The range in sDIC below 200m is much greater than that for sTA (Table 2). The lowest value is  
4  $2220 \pm 5 \mu\text{mol kg}^{-1}$  from our cruise and the highest is  $2237 \pm 3 \mu\text{mol kg}^{-1}$  from the summer  
5 JGOFS cruise (NBP 97-01). This range in sDIC concentrations below 200 m is not surprising  
6 given that sDIC concentrations vary across the input water masses. In addition, sDIC  
7 concentrations below 200 m will be influenced by carbon export particularly in summer and  
8 early autumn and over multiple seasons' air to sea flux of  $\text{CO}_2$ .

9 Assuming that deep water concentrations of TA and DIC are relatively unmodified following  
10 wintertime deep convective mixing, we estimate the  $\Omega_{\text{Ar}}$  of winter surface water by setting TA to  
11  $2338 \mu\text{mol kg}^{-1}$ , salinity to 34.5, temperature to  $-1.89^\circ\text{C}$ , phosphate to  $2.1 \mu\text{mol kg}^{-1}$ , and silicate  
12 to  $79 \mu\text{mol kg}^{-1}$ . If DIC concentrations are  $2220 \mu\text{mol kg}^{-1}$ ,  $\Omega_{\text{Ar}}$  would be 1.37. If sDIC  
13 concentrations are  $2237 \mu\text{mol kg}^{-1}$ ,  $\Omega_{\text{Ar}}$  would be 1.24 and  $\text{pCO}_2$  would be 417  $\mu\text{atm}$ .

14 These results are consistent with a study by Matson et al. (2014) where early spring  $\Omega_{\text{Ar}}$  at 20 m  
15 depth calculated using pH and salinity derived TA was 1.2 – 1.3 from Hut Point (bottom depth >  
16 200 m) and Cape Evans (bottom depth < 30 m) in McMurdo Sound. In Prydz Bay, the lowest  
17 measured winter surface  $\Omega_{\text{Ar}}$  values were also  $\sim 1.2$  for both 1993-95 (Gibson and Trull, 1999;  
18 McNeil et al., 2011) and 2010-11 (Roden et al., 2013). Weeber et al. (2015) using hydrocast data  
19 estimated that the  $\Omega_{\text{Ar}}$  of Winter Water in the Weddell Sea was  $\sim 1.3$ . In the Mertz Polynya, the  
20 lowest  $\Omega_{\text{Ar}}$  value at 100 m (below the mixed layer) was 1.2 (Shadwick et al., 2013). In Arthur  
21 Harbor on the western Antarctic Peninsula the lowest winter surface  $\Omega_{\text{Ar}}$  value was 1.31 (Schram  
22 et al., 2015).

23 A few studies find Antarctic winter  $\Omega_{\text{Ar}}$  values for surface water below 1.2. Hauri et al. (2015)  
24 used LDEO  $\text{pCO}_2$  measurements and predicted TA from salinity to estimate winter  $\Omega_{\text{Ar}}$  values of  
25 surface water in the western Antarctic Peninsula. They found that 20% of  $\Omega_{\text{Ar}}$  values were below  
26 1.2 during the spring and winter, with a few winter values near undersaturation. It is not  
27 surprising that winter surface  $\Omega_{\text{Ar}}$  values are lower in the Antarctic Peninsula than the Ross Sea  
28 given less sea ice in the Peninsula. In another study, Kapsenberg et al. (2015) report  $\Omega_{\text{Ar}}$  at 18 m  
29 depth (bottom depth < 30 m) at two coastal sites in McMurdo Sound, the Jetty and Cape Evans,  
30 for Dec-May and Nov-June respectively using pH and salinity derived TA as input variables.



1 The lowest  $\Omega_{Ar}$  observations were from May at both sites and were 1.22 and 0.96 at the Jetty and  
2 Cape Evans. The maximum calculated  $pCO_2$  was 559 at Cape Evans. The low  $\Omega_{Ar}$  and high  
3 calculated  $pCO_2$  values measured by Kapsenberg et al. (2015) may represent differences between  
4 coastal and open ocean systems—there may be a coastal amplification signal when sinking  
5 organic matter hits a shallow bed. Another possibility is that their carbon system time series,  
6 particularly at Cape Evans, is inaccurate. After conditioning and calibrating their pH  
7 measurements using discrete water samples, for logistical reasons Kapsenberg et al. (2015) could  
8 not collect additional validation samples during deployment or measure multiple carbon system  
9 parameters for crosscheck. Although the SeaFET pH sensors that they used are generally stable,  
10 they can drift (Bresnahan et al., 2014). Kapsenberg et al. (2015) have no means to assess possible  
11 pH sensor drift.

12 Following McNeil et al. (2010) and a Representative Concentration Pathway (RCP8.5) scenario  
13 (Meinshausen et al., 2011), we use the lowest  $\Omega_{Ar}$  values from 2006 ( $\Omega_{Ar} = 1.20$ ,  $pCO_2 =$   
14  $428\mu atm$ ,  $TA = 2328 \mu mol kg^{-1}$ ,  $salinity = 34.33$ ,  $SST = -1.87^\circ C$ ,  $phosphate = 2.1 \mu mol kg^{-1}$ ,  
15  $silicate = 79 \mu mol kg^{-1}$ ) to assess when the Ross Sea could become corrosive to aragonite. While  
16 shelf water salinity in the Ross Sea has declined by  $0.03 decade^{-1}$  from 1958 to 2008 (Jacobs and  
17 Giulivi, 2010), we show that such rates of change will have inconsequential effects on  $\Omega_{Ar}$ . For  
18 equilibrium conditions, surface waters in the Ross Sea would become corrosive to aragonite by  
19 2040 (2092 for calcite) when atmospheric  $CO_2$  concentrations exceed 485 ppm. In the  
20 disequilibrium scenario (McNeil et al., 2010), surface aragonite undersaturation state would  
21 occur by 2071 (2185 for calcite) when atmospheric  $CO_2$  concentrations exceed 677 ppm.

22 Mattsdotter Björk et al. (2014) also predicted the onset of summertime aragonite in the Ross Sea.  
23 Their lowest  $\Omega_{Ar}$  value was also  $\sim 1.2$  and they estimated onset of undersaturation between 2026  
24 and 2030 by increasing DIC by  $10 \mu mol kg^{-1}$  per decade. This approach does not take into  
25 account air-sea  $CO_2$  disequilibrium. In contrast, Hauck et al. (2010) found that only  $3 - 5 \mu mol$   
26  $kg^{-1}$  of anthropogenic carbon accumulated per decade between 1992 and 2008 in shelf water of  
27 the Weddell Sea. In short, our analysis suggests that it may be possible to prevent future winter  
28 aragonite undersaturation of surface waters in the Ross Sea. For instance,  $CO_2$  concentrations  
29 never exceed 543 ppm in the  $CO_2$  stabilization scenario RCP4.5 (Meinshausen et al., 2011).

1 If the Ross Sea experiences aragonite undersaturation during winter in the future, live pteropod  
2 shells would start dissolving, making them more vulnerable to predation and bacterial infection  
3 (Bednaršek et al., 2012, 2014). In particular, pteropod larvae develop during the winter/spring  
4 (Gannefors et al., 2005; Hunt et al., 2008) and their shells have been shown to completely  
5 dissolve within weeks of exposure to aragonite undersaturation (Comeau et al., 2010). Declines  
6 in pteropod populations may reduce carbon export (Manno et al., 2010) and could have dramatic  
7 ecological effects up the food web.

8 Antarctic deep sea hydrocorals may also decline or disappear at the onset of aragonite  
9 undersaturation (Shadwick et al., 2014). In addition, the shells of post-mortem bivalves and  
10 brachiopods show significant dissolution within two months of exposure to undersaturated  
11 conditions, although live organisms may be able to compensate for this dissolution (McClintock  
12 et al., 2009). For instance, Cummings et al. (2011) show that the Antarctic bivalve *Laternula*  
13 *elliptica* can increase calcification in undersaturated conditions. However, the associated energy  
14 costs may be difficult to maintain over the long term, especially for larvae. Stumpp et al. (2012)  
15 shows that while echinoid larvae can maintain calcification in high pCO<sub>2</sub> treatments, increased  
16 energetic costs reduce growth rates and ultimately increase mortality. Larvae of the Antarctic sea  
17 urchin *Sterechinus neumayeri* and seastar *Odontaster validus* are smaller and exhibit abnormal  
18 development under elevated pCO<sub>2</sub> treatments (Byrne et al., 2013; Gonzalez-Bernat et al., 2013;  
19 Yu et al., 2013). In addition, the synergistic effects of warming and OA could impact  
20 echinoderm fertilization and embryo development (Ericson et al., 2012). Although it is not clear  
21 to what extent species may acclimatize or adapt (e.g. Suckling et al., 2015), the onset of  
22 aragonite undersaturation during winter months may have profound impacts on the Ross Sea  
23 ecosystem.

24

## 25 **5 Conclusions**

26 Our study demonstrates the possibility of setting up underway TA measurement systems.  
27 Although our system was relatively unattended, carbon system crosschecks and comparisons  
28 between hydrocast and underway data indicate that our measurements were accurate. Similar  
29 underway TA systems could be set up on scientific vessels and ships of opportunity in  
30 undersampled regions of the world's oceans.

1 We find that the seasonal increase in  $\Omega_{Ar}$  in the Ross Sea by early autumn is driven almost  
2 entirely by phytoplankton photosynthesis. In the Southern Ocean between the Ross Sea and  
3 Chile we find that  $\Omega_{Ar}$  also increases mainly due to declining  $DIC_{calc}$  although declining TA  
4 partially counters the influence of declining  $DIC_{calc}$ . The influences of SST and salinity on  $\Omega_{Ar}$   
5 are minimal in the Ross Sea and on our Southern Ocean transect.

6 We establish a salinity-TA relationship for the winter that is consistent across independent  
7 datasets. Using historical  $pCO_2$  measurements from early spring along with TA predicted from  
8 salinity, we argue that it is unlikely that the Ross Sea actually experienced winter surface  $\Omega_{Ar}$   
9 values of  $\sim 1.1$  during 1996 (as per McNeal et al., 2010) and that a  $\Omega_{Ar}$  value of  $\sim 1.2$  may more  
10 accurately represent current winter conditions.

11 Since predictions are sensitive to current surface wintertime  $\Omega_{Ar}$  values as well as the extent of  
12 disequilibrium, highly accurate carbon system measurements from the winter are crucial. It is  
13 also essential to measure more than two carbon system parameters for crosscheck. For instance,  
14 pH and  $pCO_2$  sensors on moorings and floats could be used with TA predicted from salinity to  
15 calculate  $\Omega$  during the winter.

16 Our analysis indicates that the Ross Sea will not experience aragonite undersaturation until the  
17 year 2070 following RCP8.5. In some  $CO_2$  stabilization scenarios, including RCP4.5  
18 (Meinshausen et al., 2011), the Ross Sea may avoid becoming corrosive to aragonite.

19

## 20 **Acknowledgements**

21 This work was supported by the U.S. NSF (OPP-1142044 to R. B. D) and a NSF Graduate  
22 Research Fellowship grant (DGE-114747 to H. B. D). We thank the captain and crew of the *R/V*  
23 *Nathaniel B. Palmer*. We are grateful to S. Bercovici for the nitrate data. The comments of two  
24 anonymous reviewers greatly improved this paper.

25

## 26 **References**

27 Accornero, A., Manno, C., Esposito, F. and Gambi, M. C.: The vertical flux of particulate matter  
28 in the polynya of Terra Nova Bay. Part II. Biological components, *Antarct. Sci.*, 15, 175–188,  
29 doi:10.1017/S0954102003001214, 2003.

1 Andersson, A. J., Mackenzie, F. T. and Gattuso, J.-P.: Effects of ocean acidification on benthic  
2 processes, organisms, and ecosystems, in: *Ocean Acidification*, edited by: Gattuso, J.-P. and  
3 Hanson, L., Oxford University Press, New York, 122-153, 2011.

4 Archer, D., Eby, M., Brovkin, V., Ridgwell, A., Cao, L., Mikolajewicz, U., Caldeira, K.,  
5 Matsumoto, K., Munhoven, G., Montenegro, A. and Tokos, K.: Atmospheric Lifetime of Fossil  
6 Fuel Carbon Dioxide, *Annu. Rev. Earth Planet. Sci.*, 37, 117–134,  
7 doi:10.1146/annurev.earth.031208.100206, 2009.

8 Arrigo, K. R. and McClain, C. R.: Spring Phytoplankton Production in the Western Ross Sea,  
9 *Science*, 266, 261–263, doi:10.1126/science.266.5183.261, 1994.

10 Arrigo, K. R. and van Dijken, G. L.: Phytoplankton dynamics within 37 Antarctic coastal  
11 polynya systems, *J. Geophys. Res.*, 108, 3271, doi:10.1029/2002JC001739, 2003.

12 Arrigo, K. R. and Van Dijken, G. L.: Annual changes in sea-ice, chlorophyll a, and primary  
13 production in the Ross Sea, Antarctica, *Deep. Res. Part II Top. Stud. Oceanogr.*, 51, 117–138,  
14 doi:10.1016/j.dsr2.2003.04.003, 2004.

15 Arrigo, K. R. and Van Dijken, G. L.: Interannual variation in air-sea CO<sub>2</sub> flux in the Ross Sea,  
16 Antarctica: A model analysis, *J. Geophys. Res.*, 112, 1–16, doi:10.1029/2006JC003492, 2007.

17 Arrigo, K. R., Robinson, D. H., Worthen, D. L., Dunbar, R. B., DiTullio, G. R., VanWoert, M.  
18 and Lizotte, M. P.: Phytoplankton community structure and the drawdown of nutrients and CO<sub>2</sub>  
19 in the Southern Ocean, *Science*, 283, 365–367, doi:10.1126/science.283.5400.365, 1999.

20 Arrigo, K. R., Worthen, D. L. and Robinson, D. H.: A coupled ocean-ecosystem model of the  
21 Ross Sea: 2. Iron regulation of phytoplankton taxonomic variability and primary production, *J.*  
22 *Geophys. Res.*, 108, 3231, doi:10.1029/2001JC000856, 2003.

23 Arrigo, K. R., van Dijken, G. L. and Bushinsky, S.: Primary production in the Southern Ocean,  
24 1997–2006, *J. Geophys. Res.*, 113, C08004, doi:10.1029/2007JC004551, 2008.

25 Bates, N. R., Hansell, D. A., Carlson, C. A. and Gordon, L. I.: Distribution of CO<sub>2</sub> species,  
26 estimates of net community production, and air-sea CO<sub>2</sub> exchange in the Ross Sea polynya, *J.*  
27 *Geophys. Res.*, 103, 2883–2896, doi:10.1029/97jc02473, 1998.

1 Bates, N. R., Orchowka, M. I., Garley, R. and Mathis, J. T.: Summertime calcium carbonate  
2 undersaturation in shelf waters of the western Arctic Ocean – how biological processes  
3 exacerbate the impact of ocean acidification, *Biogeosciences*, 10, 5281–5309, doi:10.5194/bg-  
4 10-5281-2013, 2013.

5 Bednaršek, N., Tarling, G. a., Bakker, D. C. E., Fielding, S., Jones, E. M., Venables, H. J., Ward,  
6 P., Kuzirian, a., Lézé, B., Feely, R. a. and Murphy, E. J.: Extensive dissolution of live pteropods  
7 in the Southern Ocean, *Nat. Geosci.*, 5, 881–885, doi:10.1038/ngeo1635, 2012.

8 Bednaršek, N., Tarling, G. A., Bakker, D. C., Fielding, S. and Feely, R. A.: Dissolution  
9 dominating calcification process in polar pteropods close to the point of aragonite  
10 undersaturation, *PLoS One*, 9, e109183, doi:10.1371/journal.pone.0109183, 2014.

11 Bresnahan, P. J., Martz, T. R., Takeshita, Y., Johnson, K. S. and Lashomb, M.: Best practices for  
12 autonomous measurement of seawater pH with the Honeywell Durafet, *Methods Oceanogr.*, 9,  
13 1–33, doi:10.1016/j.mio.2014.08.003, 2014.

14 Brewer, P. G. and Goldman, J. C.: Alkalinity changes generated by phytoplankton growth,  
15 *Limnol. Oceanogr.*, 21, 108–117, doi:10.4319/lo.1976.21.1.0108, 1976.

16 Byrne, M., Ho, M. a., Koleits, L., Price, C., King, C. K., Virtue, P., Tilbrook, B. and Lamare, M.:  
17 Vulnerability of the calcifying larval stage of the Antarctic sea urchin *Sterechinus neumayeri* to  
18 near-future ocean acidification and warming, *Glob. Chang. Biol.*, 19, 2264–2275,  
19 doi:10.1111/gcb.12190, 2013.

20 Caldeira, K. and Wickett, M. E.: Oceanography: anthropogenic carbon and ocean pH., *Nature*,  
21 425, 365, doi:10.1038/425365a, 2003.

22 Chierici, M. and Fransson, A.: Calcium carbonate saturation in the surface water of the Arctic  
23 Ocean: undersaturation in freshwater influenced shelves, *Biogeosciences*, 6, 2421–2431,  
24 doi:10.5194/bg-6-2421-2009, 2009.

25 Collier, R., Dymond, J., Honjo, S., Manganini, S., Francois, R. and Dunbar, R.: The vertical flux  
26 of biogenic and lithogenic material in the Ross Sea: Moored sediment trap observations 1996-  
27 1998, *Deep. Res. Part II Top. Stud. Oceanogr.*, 47, 3491–3520, doi:10.1016/S0967-  
28 0645(00)00076-X, 2000.

1 Comeau, S., Gorsky, G., Alliouane, S., Gattuso, J.-P. and 10.1594/PANGAEA.733905: Larvae  
2 of the pteropod *Cavolinia inflexa* exposed to aragonite undersaturation are viable but shell-less,  
3 *Mar. Biol.*, 157, 2341–2345, doi:10.1007/s00227-010-1493-6, 2010.

4 Cummings, V., Hewitt, J., Van Rooyen, A., Currie, K., Beard, S., Thrush, S., Norkko, J., Barr,  
5 N., Heath, P., Halliday, N. J., Sedcole, R., Gomez, A., McGraw, C. and Metcalf, V.: Ocean  
6 acidification at high latitudes: potential effects on functioning of the Antarctic bivalve *Laternula*  
7 *elliptica*, *PLoS ONE*, 6, e16069, doi:10.1371/journal.pone.0016069, 2011.

8 Dickson, A. G.: The carbon dioxide system in seawater: equilibrium chemistry and  
9 measurements, in: *Guide to Best Practices in Ocean Acidification Research and Data Reporting*,  
10 edited by: Riebesell, U., Fabry, V. J., Hansson, L., and Gattuso, J.-P., Luxembourg, Office for  
11 Official Publications of the European Communities, 17–40, 2010.

12 Dickson, A. G., and Millero, F. J.: A comparison of the equilibrium constants for the dissociation  
13 of carbonic acid in seawater media, *Deep Sea Res. Part A. Oceanogr. Res. Pap.*, 34, 1733–1743,  
14 doi:10.1016/0198-0149(87)90021-5, 1987.

15 Dickson, A. G., Afghan, J. D. and Anderson, G. C.: Reference materials for oceanic CO<sub>2</sub>  
16 analysis: a method for the certification of total alkalinity, *Mar. Chem.*, 80, 185–197,  
17 doi:10.1016/S0304-4203(02)00133-0, 2003.

18 Dickson, A. G., Sabine, C. L. and Christian, J. R.: *Guide to best practices for ocean CO<sub>2</sub>*  
19 *measurements*, *PICES Spec. Publ.*, 3, p191, doi:10.1159/000331784, 2007.

20 Dieckmann, G. S., Nehrke, G., Papadimitriou, S., Göttlicher, J., Steininger, R., Kennedy, H.,  
21 Wolf-Gladrow, D. and Thomas, D. N.: Calcium carbonate as ikaite crystals in Antarctic sea ice,  
22 *Geophys. Res. Lett.*, 35, 35–37, doi:10.1029/2008GL033540, 2008.

23 Dinniman, M. S., Klinck, J. M. and Smith, W. O.: A model study of Circumpolar Deep Water on  
24 the West Antarctic Peninsula and Ross Sea continental shelves, *Deep Sea Res. Part II Top. Stud.*  
25 *Oceanogr.*, 58, 1508–1523, doi:10.1016/j.dsr2.2010.11.013, 2011.

26 Ericson, J. A., Ho, M. A., Miskelly, A., King, C. K., Virtue, P., Tilbrook, B. and Byrne, M.:  
27 Combined effects of two ocean change stressors, warming and acidification, on fertilization and  
28 early development of the Antarctic echinoid *Sterechinus neumayeri*, *Polar Biol.*, 35, 1027–1034,  
29 doi:10.1007/s00300-011-1150-7, 2012.

1 Feely, R., Doney, S. and Cooley, S.: Ocean Acidification: Present Conditions and Future  
2 Changes in a High-CO<sub>2</sub> World, *Oceanography*, 22, 36–47, doi:10.5670/oceanog.2009.95, 2009.

3 Feng, Y., Hare, C. E., Rose, J. M., Handy, S. M., DiTullio, G. R., Lee, P. A., Smith, W. O.,  
4 Peloquin, J., Tozzi, S., Sun, J., Zhang, Y., Dunbar, R. B., Long, M. C., Sohst, B., Lohan, M. and  
5 Hutchins, D. A.: Interactive effects of iron, irradiance and CO<sub>2</sub> on Ross Sea phytoplankton,  
6 *Deep. Res. Part I Oceanogr. Res. Pap.*, 57, 368–383, doi:10.1016/j.dsr.2009.10.013, 2010.

7 Foster, B. A. and Montgomery, J. C.: Planktivory in benthic nototheniid fish in McMurdo Sound,  
8 Antarctica, *Environ. Biol. Fishes*, 36, 313–318, doi:10.1007/BF00001727, 1993.

9 Fransson, A., Chierici, M., Yager, P. L. and Smith, W. O.: Antarctic sea ice carbon dioxide  
10 system and controls, *J. Geophys. Res.*, 116, C12035, doi:10.1029/2010JC006844, 2011.

11 Gannefors, C., Boer, M., Kattner, G., Graeve, M., Eiane, K., Gulliksen, B., Hop, H. and Falk-  
12 Petersen, S.: The Arctic sea butterfly *Limacina helicina*: lipids and life strategy, *Mar. Biol.*, 147,  
13 169–177, doi:10.1007/s00227-004-1544-y, 2005.

14 Gibson, J. A. . E. and Trull, T. W.: Annual cycle of fCO<sub>2</sub> under sea-ice and in open water in  
15 Prydz Bay, East Antarctica, *Mar. Chem.*, 66, 187–200, doi:10.1016/S0304-4203(99)00040-7,  
16 1999.

17 Gonzalez-Bernat, M. J., Lamare, M. and Barker, M.: Effects of reduced seawater pH on  
18 fertilisation, embryogenesis and larval development in the Antarctic seastar *Odontaster validus*,  
19 *Polar Biol.*, 36, 235–247, doi:10.1007/s00300-012-1255-7, 2013.

20 Gordon, L. I., Codispoti, L. A., Jennings J.C., J., Millero, F. J., Morrison, J. M. and Sweeney, C.:  
21 Seasonal evolution of hydrographic properties in the Ross Sea, Antarctica, 1996-1997, *Deep.*  
22 *Res. Part II Top. Stud. Oceanogr.*, 47, 3095–3117, doi:10.1016/S0967-0645(00)00060-6, 2000.

23 Hauck, J., Hoppema, M., Bellerby, R. G. J., Völker, C. and Wolf-Gladrow, D.: Data-based  
24 estimation of anthropogenic carbon and acidification in the Weddell Sea on a decadal timescale,  
25 *J. Geophys. Res. Ocean.*, 115, 1–14, doi:10.1029/2009JC005479, 2010.

26 Hauck, J., Arrigo, K. R., Hoppema, M., Van Dijken, G. L., Völker, C. and Wolf-Gladrow, D. A.:  
27 Insignificant buffering capacity of Antarctic shelf carbonates, *Global Biogeochem. Cycles*, 27,  
28 11–20, doi:10.1029/2011GB004211, 2013.

1 Hauri, C., Gruber, N., Vogt, M., Doney, S. C., Feely, R. A., Lachkar, Z., Leinweber, A.,  
2 McDonnell, A. M. P. and Munnich, M.: Spatiotemporal variability and long-term trends of ocean  
3 acidification in the California Current System, *Biogeosciences*, 10, 193–216, doi:10.5194/bg-10-  
4 193-2013, 2013.

5 Hauri, C., Doney, S. C., Takahashi, T., Erickson, M., Jiang, G. and Ducklow, H. W.: Two  
6 decades of inorganic carbon dynamics along the Western Antarctic Peninsula, *Biogeosciences*  
7 *Discuss.*, 12, 6929–6969, doi:10.5194/bgd-12-6929-2015, 2015.

8 Hopkins, T. L.: Midwater food web in McMurdo Sound, Ross Sea, Antarctica, *Mar. Biol.*, 96,  
9 93–106, doi:10.1007/BF00394842, 1987.

10 Hunt, B. P. V., Pakhomov, E. A., Hosie, G. W., Siegel, V., Ward, P. and Bernard, K.: Pteropods  
11 in Southern Ocean ecosystems, *Prog. Oceanogr.*, 78, 193–221,  
12 doi:10.1016/j.pocean.2008.06.001, 2008.

13 IPCC AR5 WG1 (2013), *Climate Change 2013: The Physical Science Basis. Contribution of*  
14 *Working Group I to the Fifth Assessment Report of the Intergovernmental Panel on Climate*  
15 *Change Rep.*, 1535 pp, Cambridge, United Kingdom and New York, NY, USA.

16 Jacobs, S. S.: On the nature and significance of the Antarctic Slope Front, *Mar. Chem.*, 35, 9–24,  
17 doi:10.1016/S0304-4203(09)90005-6, 1991.

18 Jacobs, S. S. and Giulivi, C. F.: Large multidecadal salinity trends near the Pacific-Antarctic  
19 continental margin, *J. Clim.*, 23, 4508–4524, doi:10.1175/2010JCLI3284.1, 2010.

20 Jacobs, S. S., Fairbanks, R. G., Horibe, Y.: Origin and evolution of water masses near the  
21 Antarctic continental margin: evidence from  $\text{H}_2^{18}\text{O}/\text{H}_2^{16}\text{O}$  ratios in seawater, in: *Oceanography*  
22 *of the Antarctic Continental Shelf, Antarctic Research Series*, 43, edited by: Jacobs, S. S.,  
23 American Geophysical Union, Washington, D.C, 59–85, 1985.

24 Kapsenberg, L., Kelley, A. L., Shaw, E. C., Martz, T. R. and Hofmann, G. E.: Near-shore  
25 Antarctic pH variability has implications for the design of ocean acidification experiments, *Sci.*  
26 *Rep.*, 5, 9638, doi:10.1038/srep09638, 2015.



1 Kawaguchi, S., Ishida, A., King, R., Raymond, B., Waller, N., Constable, A., Nicol, S., Wakita,  
2 M. and Ishimatsu, A.: Risk maps for Antarctic krill under projected Southern Ocean  
3 acidification, *Nat. Clim. Chang.*, 3, 843–847, doi:10.1038/nclimate1937, 2013.

4 Knap, A., Michaels A., Close A., Ducklow, H. and A. Dickson: Protocols for the Joint Global  
5 Ocean Flux Study ( JGOFS ) Core Measurements, JGOFS Rep., 19, 1–170, 1996.

6 Kohut, J., Hunter, E. and Huber, B.: Small-scale variability of the cross-shelf flow over the outer  
7 shelf of the Ross Sea, *J. Geophys. Res. Ocean.*, 118, 1863–1876, doi:10.1002/jgrc.20090, 2013.

8 La Mesa, M., Vacchi, M. and Zunini Sertorio, T.: Feeding plasticity of *Trematomus newnesi*  
9 (Pisces, Nototheniidae) in Terra Nova Bay, Ross Sea, in relation to environmental conditions,  
10 *Polar Biol.*, 23, 38–45, doi:10.1007/s003000050006, 2000.

11 La Mesa, M., Eastman, J. T. and Vacchi, M.: The role of notothenioid fish in the food web of the  
12 Ross Sea shelf waters: A review, *Polar Biol.*, 27, 321–338, doi:10.1007/s00300-004-0599-z,  
13 2004.

14 Lee, K., Millero, F. J., Byrne, R. H., Feely, R. A. and Wanninkhof, R.: The recommended  
15 dissociation constants for carbonic acid in seawater, *Geophys. Res. Lett.*, 27, 229,  
16 doi:10.1029/1999GL002345, 2000.

17 Lenton, A., Codron, F., Bopp, L., Metzl, N., Cadule, P., Tagliabue, A. and Le Sommer, J.:  
18 Stratospheric ozone depletion reduces ocean carbon uptake and enhances ocean acidification,  
19 *Geophys. Res. Lett.*, 36, L12606, doi:10.1029/2009GL038227, 2009.

20 Lewis, E. and Wallace, D. W. R.: Program Developed for CO<sub>2</sub> System Calculations  
21 ORNL/CDIAC-105, Carbon Dioxide Information Analysis Centre, Oak Ridge National  
22 Laboratory, US Department of Energy, Tennessee, 1998.

23 Long, M. C., Dunbar, R. B., Tortell, P. D., Smith, W. O., Mucciarone, D. a. and Ditullio, G. R.:  
24 Vertical structure, seasonal drawdown, and net community production in the Ross Sea,  
25 Antarctica, *J. Geophys. Res. Ocean.*, 116, 1–19, doi:10.1029/2009JC005954, 2011.

26 Manno, C., Tirelli, V., Accornero, A. and Fonda Umani, S.: Importance of the contribution of  
27 limacina helicina faecal pellets to the carbon pump in terra nova bay (Antarctica), *J. Plankton*  
28 *Res.*, 32, 145–152, doi:10.1093/plankt/fbp108, 2010.

1 Matson, P. G., Washburn, L., Martz, T. R. and Hofmann, G. E.: Abiotic versus Biotic Drivers of  
2 Ocean pH Variation under Fast Sea Ice in McMurdo Sound, Antarctica, 9, e107239,  
3 doi:10.1371/journal.pone.0107239, 2014.

4 Mattsdotter Björk, M., Fransson, A., Torstensson, A. and Chierici, M.: Ocean acidification state  
5 in western Antarctic surface waters: Controls and interannual variability, Biogeosciences, 11,  
6 57–73, doi:10.5194/bg-11-57-2014, 2014.

7 McClintock, J. B., Angus, R. a., Mcdonald, M. R., Amsler, C. D., Catledge, S. a. and Vohra, Y.  
8 K.: Rapid dissolution of shells of weakly calcified antarctic benthic macroorganisms indicates  
9 high vulnerability to ocean acidification, Antarct. Sci., 21, 449–456,  
10 doi:10.1017/S0954102009990198, 2009.

11 McClintock, J. B., Amsler, M. O., Angus, R. A., Challener, R. C., Schram, J. B., Amsler, C. D.,  
12 Mah, C. L., Cuce, J. and Baker, B. J.: The Mg-Calcite Composition of Antarctic Echinoderms:  
13 Important Implications for Predicting the Impacts of Ocean Acidification, J. Geol., 119, 457–  
14 466, doi:10.1086/660890, 2011.

15 McNeil, B. I. and Matear, R. J.: Southern Ocean acidification: a tipping point at 450-ppm  
16 atmospheric CO<sub>2</sub>, Proc. Natl. Acad. Sci. U. S. A., 105, 18860–18864,  
17 doi:10.1073/pnas.0806318105, 2008.

18 McNeil, B. I., Metzl, N., Key, R. M., Matear, R. J. and Corbiere, A.: An empirical estimate of  
19 the Southern Ocean air-sea CO<sub>2</sub> flux, Global Biogeochem. Cycles, 21, GB3011,  
20 doi:10.1029/2007GB002991, 2007.

21 McNeil, B. I., Tagliabue, A. and Sweeney, C.: A multi-decadal delay in the onset of corrosive  
22 acidified waters in the Ross Sea of Antarctica due to strong air-sea CO<sub>2</sub> disequilibrium, Geophys.  
23 Res. Lett., 37, 1–5, doi:10.1029/2010GL044597, 2010.

24 McNeil, B. I., Sweeney, C. and Gibson, J. A. E.: Short Note: Natural seasonal variability of  
25 aragonite saturation state within two Antarctic coastal ocean sites, Antarct. Sci., 23, 411–412,  
26 doi:10.1017/S0954102011000204, 2011.

27 Mehrback, C., Culberson, C. H., Hawley, J. E. and Pytkowicz, R. M.: Measurement of the  
28 apparent dissociation constants of carbonic acid in seawater at atmospheric pressure, Limnol.  
29 Oceanogr., 18, 897–907, doi:10.4319/lo.1973.18.6.0897, 1973.

1 Metzl, N., Brunet, C., Jabaud-Jan, A., Poisson, A. and Schauer, B.: Summer and winter air-sea  
2 CO<sub>2</sub> fluxes in the Southern Ocean, *Deep. Res. Part I Oceanogr. Res. Pap.*, 53, 1548–1563,  
3 doi:10.1016/j.dsr.2006.07.006, 2006.

4 Millero, F. J., Lee, K. and Roche, M.: Distribution of alkalinity in the surface waters of the major  
5 oceans, in *Marine Chemistry*, 60, 111–130, 1998.

6 Millero, F. J., Pierrot, D., Lee, K., Wanninkhof, R., Feely, R., Sabine, C. L., Key, R. M. and  
7 Takahashi, T.: Dissociation constants for carbonic acid determined from field measurements,  
8 *Deep. Res. Part I Oceanogr. Res. Pap.*, 49, 1705–1723, doi:10.1016/S0967-0637(02)00093-6,  
9 2002.

10 Moy, A. D., Howard, W. R., Bray, S. G. and Trull, T. W.: Reduced calcification in modern  
11 Southern Ocean planktonic foraminifera, *Nat. Geosci.*, 2, 276–280, doi:10.1038/ngeo460, 2009.

12 Mucci, A.: The solubility of calcite and aragonite in seawater at various salinities, temperatures,  
13 and one atmosphere total pressure., *Am. J. Sci.*, 283, 780–799, doi:10.2475/ajs.283.7.780, 1983.

14 Orr, J. C., Fabry, V. J., Aumont, O., Bopp, L., Doney, S. C., Feely, R. A., Gnanadesikan, A.,  
15 Gruber, N., Ishida, A., Joos, F., Key, R. M., Lindsay, K., Maier-Reimer, E., Matear, R., Monfray,  
16 P., Mouchet, A., Najjar, R. G., Plattner, G.-K., Rodgers, K. B., Sabine, C. L., Sarmiento, J. L.,  
17 Schlitzer, R., Slater, R. D., Totterdell, I. J., Weirig, M.-F., Yamanaka, Y. and Yool, A.:  
18 Anthropogenic ocean acidification over the twenty-first century and its impact on calcifying  
19 organisms., *Nature*, 437, 681–686, doi:10.1038/nature04095, 2005.

20 Orsi, A. H. and Wiederwohl, C. L.: A recount of Ross Sea waters, *Deep Sea Res. Part II Top.*  
21 *Stud. Oceanogr.*, 56, 778–795, doi:10.1016/j.dsr2.2008.10.033, 2009.

22 Orsi, A. H., Whitworth, T. and Nowlin, W. D.: On the meridional extent and fronts of the  
23 Antarctic Circumpolar Current, *Deep Sea Res. Part I Oceanogr. Res. Pap.*, 42, 641–673,  
24 doi:10.1016/0967-0637(95)00021-W, 1995.

25 Petty, a. a., Holland, P. R. and Feltham, D. L.: Sea ice and the ocean mixed layer over the  
26 Antarctic shelf seas, *Cryosphere*, 8, 761–783, doi:10.5194/tc-8-761-2014, 2014.

27 Reuer, M. K., Barnett, B. A., Bender, M. L., Falkowski, P. G. and Hendricks, M. B.: New  
28 estimates of Southern Ocean biological production rates from O<sub>2</sub>/Ar ratios and the triple isotope

1 composition of O<sub>2</sub>, *Deep. Res. Part I Oceanogr. Res. Pap.*, 54, 951–974,  
2 doi:10.1016/j.dsr.2007.02.007, 2007.

3 Riebesell, U., Zondervan, I., Rost, B., Tortell, P. D., Zeebe, R. E. and Morel, F. M.: Reduced  
4 calcification of marine plankton in response to increased atmospheric CO<sub>2</sub>, *Nature*, 407, 364–7,  
5 doi:10.1038/35030078, 2000.

6 Rintoul, S., Hughes, C. and Olbers, D.: The Antarctic Circumpolar Current System BT - Ocean  
7 Circulation and Climate, in: *Ocean Circulation and Climate*, 271–301, 2001.

8 Rivaro, P., Messa, R., Ianni, C., Magi, E. and Budillon, G.: Distribution of total alkalinity and  
9 pH in the Ross Sea (Antarctica) waters during austral summer 2008, *Polar Res.*, 33, 269,  
10 doi:10.3402/polar.v33.20403, 2014.

11 Robbins, L. L., Wynn, J. G., Lisle, J. T., Yates, K. K., Knorr, P. O., Byrne, R. H., Liu, X.,  
12 Patsavas, M. C., Azetsu-Scott, K. and Takahashi, T.: Baseline monitoring of the western Arctic  
13 Ocean estimates 20% of Canadian basin surface waters are undersaturated with respect to  
14 aragonite., *PLoS One*, 8, e73796, doi:10.1371/journal.pone.0073796, 2013.

15 Roden, N. P., Shadwick, E. H., Tilbrook, B. and Trull, T. W.: Annual cycle of carbonate  
16 chemistry and decadal change in coastal Prydz Bay, East Antarctica, *Mar. Chem.*, 155, 135–147,  
17 doi:10.1016/j.marchem.2013.06.006, 2013.

18 Rubin, S. I.: Carbon and nutrient cycling in the upper water column across the Polar Frontal  
19 Zone and Antarctic Circumpolar Current along 170°W, *Global Biogeochem. Cycles*, 17, 1087,  
20 doi:10.1029/2002GB001900, 2003.

21 Rubin, S. I., Takahashi, T., Chipman, D. W. and Goddard, J. G.: Primary productivity and  
22 nutrient utilization ratios in the Pacific sector of the Southern Ocean based on seasonal changes  
23 in seawater chemistry, *Deep. Res. Part I Oceanogr. Res. Pap.*, 45, 1211–1234,  
24 doi:10.1016/S0967-0637(98)00021-1, 1998.

25 Saenz, B. T. and Arrigo, K. R.: Annual primary production in Antarctic sea ice during 2005-  
26 2006 from a sea ice state estimate, *J. Geophys. Res. Ocean.*, 119, 3645–3678,  
27 doi:10.1002/2013JC009677, 2014.

1 Sandrini, S., Ait-Ameur, N., Rivaro, P., Massolo, S., Touratier, F., Tositti, L. and Goyet, C.:  
2 Anthropogenic carbon distribution in the Ross Sea, Antarctica, *Antarct. Sci.*, 19, 395–407,  
3 doi:10.1017/S0954102007000405, 2007.

4 Schram, J. B., Schoenrock, K. M., McClintock, J. B., Amsler, C. D. and Angus, R. a.: Multi-  
5 frequency observations of seawater carbonate chemistry on the central coast of the western  
6 Antarctic Peninsula, *Polar Res.*, 1, 1–49, 2015.

7 Seibel, B. A. and Dierssen, H. M.: Cascading Trophic Impacts of Reduced Biomass in the Ross  
8 Sea, Antarctica: Just the Tip of the Iceberg?, *Biol. Bull.*, 205, 93–97, 2003.

9 Sewell, M. A. and Hofmann, G. E.: Antarctic echinoids and climate change: A major impact on  
10 the brooding forms, *Glob. Chang. Biol.*, 17, 734–744, doi:10.1111/j.1365-2486.2010.02288.x,  
11 2011.

12 Shadwick, E. H., Rintoul, S. R., Tilbrook, B., Williams, G. D., Young, N., Fraser, a. D.,  
13 Marchant, H., Smith, J. and Tamura, T.: Glacier tongue calving reduced dense water formation  
14 and enhanced carbon uptake, *Geophys. Res. Lett.*, 40, 904–909, doi:10.1002/grl.50178, 2013.

15 Shadwick, E. H., Tilbrook, B. and Williams, G. D.: Carbonate chemistry in the Mertz Polynya  
16 (East Antarctica): Biological and physical modification of dense water outflows and the export  
17 of anthropogenic CO<sub>2</sub>, *J. Geophys. Res. Ocean.*, 119, 1–14, doi:10.1002/2013JC009286, 2014.

18 Smith, W. O. and Gordon, L. I.: Hyperproductivity of the Ross Sea (Antarctica) polynya during  
19 austral spring, *Geophys. Res. Lett.*, 24, 233, doi:10.1029/96GL03926, 1997.

20 Smith, W., Sedwick, P., Arrigo, K., Ainley, D. and Orsi, A.: The Ross Sea in a Sea of Change,  
21 *Oceanography*, 25, 90–103, doi:http://dx.doi.org/10.5670/oceanog.2012.80, 2012.

22 Sokolov, S. and Rintoul, S. R.: Circumpolar structure and distribution of the antarctic  
23 circumpolar current fronts: 1. Mean circumpolar paths, *J. Geophys. Res. Ocean.*, 114, 1–19,  
24 doi:10.1029/2008JC005108, 2009.

25 Spreen, G., Kaleschke, L. and Heygster, G.: Sea ice remote sensing using AMSR-E 89-GHz  
26 channels, *J. Geophys. Res. Ocean.*, 113, C02S03, doi:10.1029/2005JC003384, 2008.

27 Stumpp, M., Hu, M. Y., Melzner, F., Gutowska, M. A., Dorey, N., Himmerkus, N., Holtmann,  
28 W. C., Dupont, S. T., Thorndyke, M. C. and Bleich, M.: Acidified seawater impacts sea urchin

1 larvae pH regulatory systems relevant for calcification., Proc. Natl. Acad. Sci. U. S. A., 109,  
2 18192–7, doi:10.1073/pnas.1209174109, 2012.

3 Suckling, C. C., Clark, M. S., Richard, J., Morley, S. a., Thorne, M. a. S., Harper, E. M. and  
4 Peck, L. S.: Adult acclimation to combined temperature and pH stressors significantly enhances  
5 reproductive outcomes compared to short-term exposures, J. Anim. Ecol., 84, 773–784,  
6 doi:10.1111/1365-2656.12316, 2015.

7 Sweeney, C.: The Annual Cycle of Surface Water CO<sub>2</sub> and O<sub>2</sub> in the Ross Sea : A model for Gas  
8 Exchange on the Continental Shelves of Antarctica, in: Biogeochemistry of the Ross Sea, 295–  
9 310. 2003.

10 Sweeney, C., Hansell, D. A., Carlson, C. A., Codispoti, L. A., Gordon, L. I., Marra, J., Millero,  
11 F. J., Smith, W. O. and Takahashi, T.: Biogeochemical regimes, net community production and  
12 carbon export in the Ross Sea, Antarctica, Deep. Res. Part II Top. Stud. Oceanogr., 47, 3369–  
13 3394, doi:10.1016/S0967-0645(00)00072-2, 2000a.

14 Sweeney, C., Smith, W. O., Hales, B., Bidigare, R. R., Carlson, C. A., Codispoti, L. A., Gordon,  
15 L. I., Hansell, D. A., Millero, F. J., Park, M. O. and Takahashi, T.: Nutrient and carbon removal  
16 ratios and fluxes in the Ross Sea, Antarctica, Deep. Res. Part II Top. Stud. Oceanogr., 47, 3395–  
17 3421, doi:10.1016/S0967-0645(00)00073-4, 2000b.

18 Swift, J .H., Orsi, A. H.: Sixty-four days of hydrography and storms: RVIB Nathaniel B.  
19 Palmer’s 2011 SO4P Cruise, Oceanography, 25, 54–55, doi:10.5670/oceanog.2012.74, 2012.

20 Tagliabue, A. and Arrigo, K. R.: Iron in the Ross Sea: 1. Impact on CO<sub>2</sub> fluxes via variation in  
21 phytoplankton functional group and non-Redfield stoichiometry, J. Geophys. Res. C Ocean.,  
22 110, 1–15, doi:10.1029/2004JC002531, 2005.

23 Takahashi, T., Sutherland, S. C., Wanninkhof, R., Sweeney, C., Feely, R. A., Chipman, D. W.,  
24 Hales, B., Friederich, G., Chavez, F., Sabine, C., Watson, A., Bakker, D. C. E., Schuster, U.,  
25 Metzl, N., Yoshikawa-Inoue, H., Ishii, M., Midorikawa, T., Nojiri, Y., Körtzinger, A., Steinhoff,  
26 T., Hoppema, M., Olafsson, J., Arnarson, T. S., Tilbrook, B., Johannessen, T., Olsen, A.,  
27 Bellerby, R., Wong, C. S., Delille, B., Bates, N. R. and de Baar, H. J. W.: Climatological mean  
28 and decadal change in surface ocean pCO<sub>2</sub>, and net sea-air CO<sub>2</sub> flux over the global oceans,  
29 Deep. Res. Part II Top. Stud. Oceanogr., 56, 554–577, doi:10.1016/j.dsr2.2008.12.009, 2009.

1 Tortell, P. D., Payne, C. D., Li, Y., Trimborn, S., Rost, B., Smith, W. O., Riesselman, C.,  
2 Dunbar, R. B., Sedwick, P. and DiTullio, G. R.: CO<sub>2</sub> sensitivity of Southern Ocean  
3 phytoplankton, *Geophys. Res. Lett.*, 35, L04605, doi:10.1029/2007GL032583, 2008.

4 van Heuven, S., Pierrot, D., Rae, J. W. B., Lewis, E., and Wallace, D. W. R.: MATLAB program  
5 developed for CO<sub>2</sub> system calculations, ORNL/CDIAC-105b, Carbon Dioxide Information  
6 Analysis Center, Oak Ridge National Laboratory, US Department of Energy, Oak Ridge,  
7 Tennessee, doi:10.3334/CDIAC/otg.CO2SYS MATLAB v1.1, 2011.

8 Weeber, a., Swart, S. and Monteiro, P. M. S.: Seasonality of sea ice controls interannual  
9 variability of summertime  $\Omega$  at the ice shelf in the  
10 Eastern Weddell Sea – an ocean acidification sensitivity study, *Biogeosciences*  
11 *Discuss.*, 12, 1653–1687, doi:10.5194/bgd-12-1653-2015, 2015.

12 Yamamoto-Kawai, M., McLaughlin, F. A., Carmack, E. C., Nishino, S. and Shimada, K.:  
13 Aragonite undersaturation in the Arctic Ocean: effects of ocean acidification and sea ice melt,  
14 *Science*, 326, 1098–1100, doi:10.1126/science.1174190, 2009.

15 Yu, P. C., Sewell, M. a., Matson, P. G., Rivest, E. B., Kapsenberg, L. and Hofmann, G. E.:  
16 Growth attenuation with developmental schedule progression in embryos and early larvae of  
17 *Sterechinus neumayeri* raised under elevated CO<sub>2</sub>, *PLoS One*, 8, e52448,  
18 doi:10.1371/journal.pone.0052448, 2013.

19  
20  
21  
22  
23  
24  
25  
26  
27  
28

1 **Table 1.** Mean values for sDIC concentrations below 200 m

| Data source              | Early Spring | Spring   | Summer   | Autumn   |
|--------------------------|--------------|----------|----------|----------|
| Sweeney et al.<br>(2000) | 2226 ± 3     | 2233 ± 3 | 2237 ± 3 | 2233 ± 5 |
| Long et al.<br>(2011 )   |              | 2224 ± 5 | 2225 ± 4 |          |
| This paper               |              |          |          | 2220 ± 5 |

2



1 **Table 2.** Water properties of CDW from McNeil et al. (2010) and CLIVAR

| Data source          | Salinity     | DIC ( $\mu\text{mol kg}^{-1}$ ) | TA ( $\mu\text{mol kg}^{-1}$ ) | PO <sub>4</sub> ( $\mu\text{mol kg}^{-1}$ ) | SiO <sub>4</sub> ( $\mu\text{mol kg}^{-1}$ ) | $\Omega_{\text{Ar}}$ |
|----------------------|--------------|---------------------------------|--------------------------------|---|--|----------------------|
| McNeil et al. (2010) | 34.70 ± 0.02 | 2255 ± 1                        | 2330                           | 2.22 ± 0.01                                 | 93.5 ± 1.2                                   | 1.01                 |
| CLIVAR               | 34.71 ± 0.02 | 2257 ± 3                        | 2348 ± 4                       | 2.21 ± 0.04                                 | 95.6 ± 6.0                                   | 1.18                 |

1 **Fig. 1.** Maps of (a) 6.25 km gridded sea ice concentration on 1 Dec 2012 from the University of  
2 Bremen, <http://www.iup.uni-bremen.de:8084/amsr2/#Antarctic> (Spren et al., 2008), (b) sea  
3 surface salinity from NBP 13-02, (c) satellite chlorophyll concentration on Feb 2013 from the 9  
4 km level 3 Aqua MODIS product, <http://oceancolor.gsfc.nasa.gov/cgi/13>, (d) sTA from NBP 13-  
5 02, (e) pCO<sub>2</sub> from NBP 13-02 (f) aragonite saturation state ( $\Omega_{Ar}$ ) from NBP 13-02.

6  
7 **Fig. 2.** Cruise track (black line) from NBP 13-02. Stations used in this study (red circles) from  
8 (a) TRACERS (NBP 13-02) and (b) CLIVAR (NBP 11-02). Blue line is the 1000 m isobath.

9  
10 **Fig. 3.** Contributions of sDIC, sTA, temperature, salinity, and PALK to changes in the aragonite  
11 saturation state ( $\Omega_{Ar}$ ) of surface waters from the winter to early autumn. Error bars represent  $\pm 1$   
12 S.D.

13  
14 **Fig. 4.** Surface water properties from a Southern Ocean transect, 20 March – 2 April 2013: (a)  
15 aragonite saturation state ( $\Omega_{Ar}$ ), (b) SST, (c) pCO<sub>2</sub>, and (d) particulate organic carbon. The  
16 locations of the Subantarctic Front (SAF), the Polar Front (PF), and the southern Antarctic  
17 Circumpolar Current Front (SACCF) from Sokolov and Rintoul (2009) are indicated (grey lines).

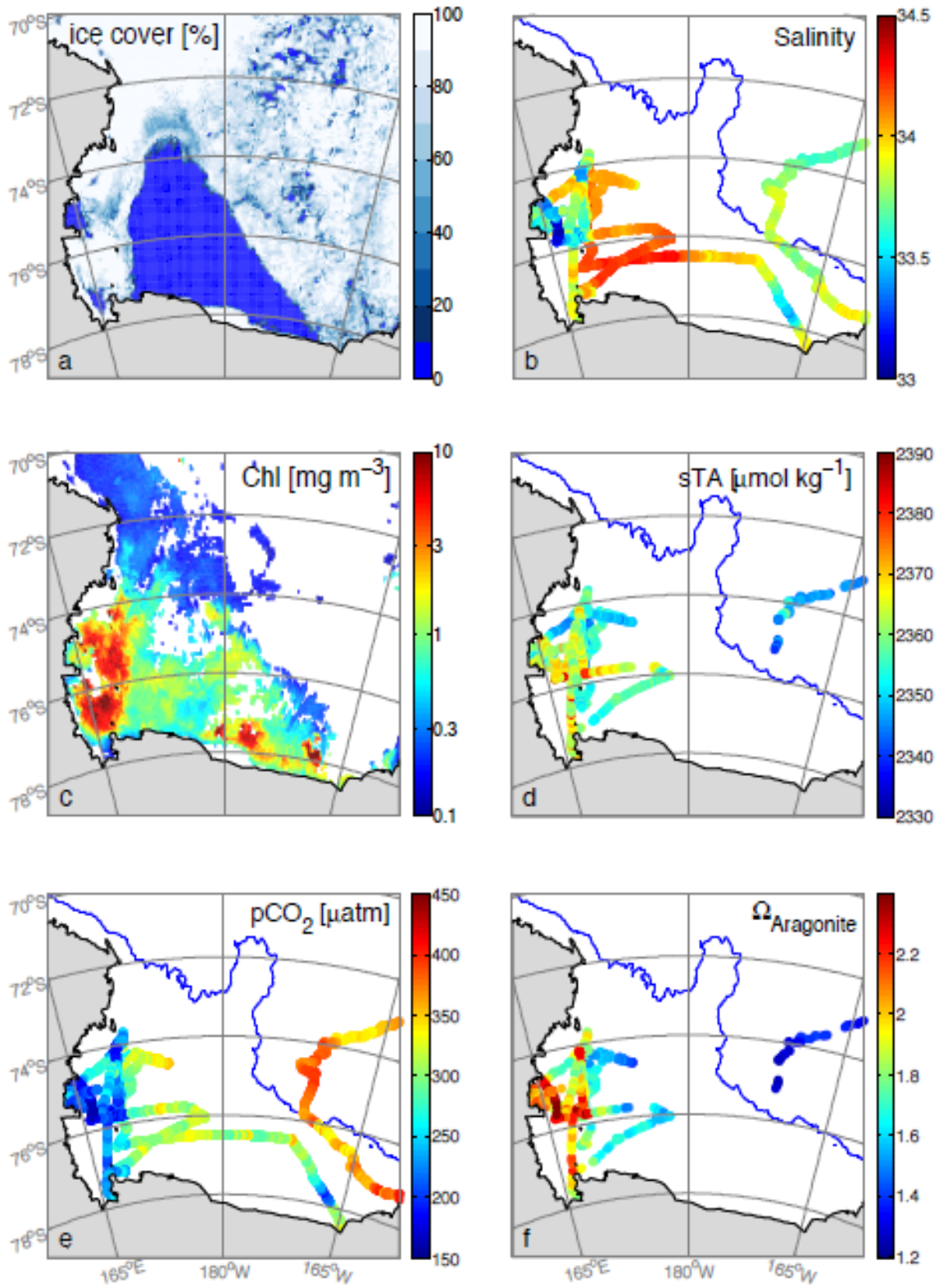
18  
19 **Fig. 5.** From surface water measurements along a Southern Ocean transect (a) contributions of  
20 changing sDIC (red), sTA (blue), temperature (green), and salinity (magenta) to changing  
21 aragonite saturation state (black,  $\Omega_{Ar}$ ) relative to the start of the transect and (b) TA to DIC  
22 ratios. The locations of the Subantarctic Front (SAF), the Polar Front (PF), and the southern  
23 Antarctic Circumpolar Current Front (SACCF) from Sokolov and Rintoul (2009) are indicated  
24 (grey lines).

25  
26 **Fig. 6.** Measured surface water salinity normalized (a) DIC calculated from pCO<sub>2</sub>, TA,  
27 temperature, and salinity and (b) TA. The locations of the Subantarctic Front (SAF), the Polar  
28 Front (PF), and the southern Antarctic Circumpolar Current Front (SACCF) from Sokolov and  
29 Rintoul (2009) are indicated (grey lines).

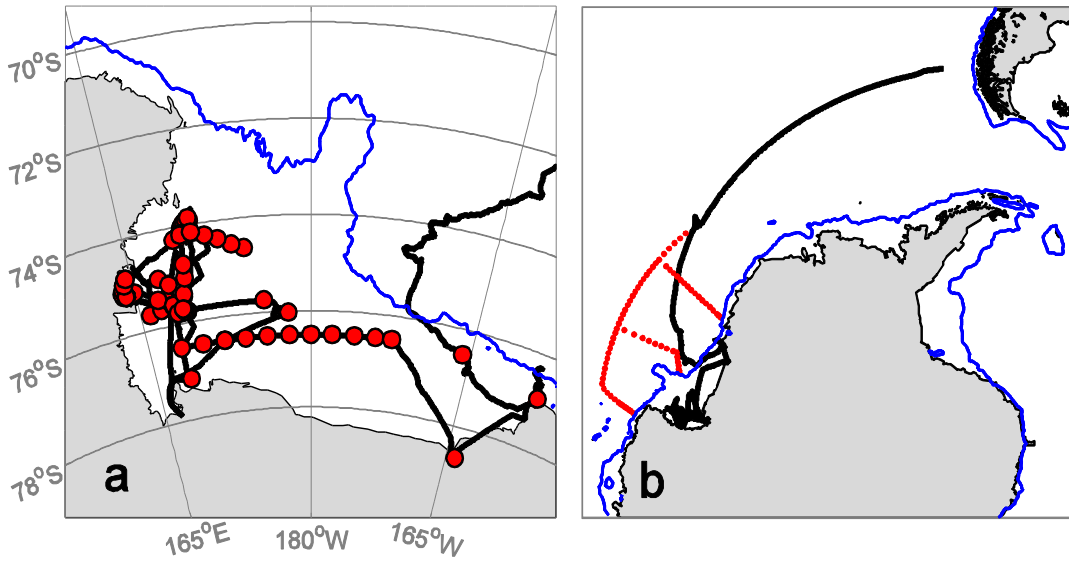
30

1 **Fig. 7.** Estimating winter surface aragonite saturation states ( $\Omega_{Ar}$ ): **(a)** map of surface pCO<sub>2</sub>  
2 measurements from the LDEO pCO<sub>2</sub> database (<http://www.ldeo.columbia.edu/res/pi/CO2>) used  
3 in this study from November 1994 (blue), 1997 (red), 2005 (green), and 2006 (black). Blue line  
4 is the 1000 m isobath. **(b)** aragonite saturation state ( $\Omega_{Ar}$ ) of surface waters from November  
5 calculated from pCO<sub>2</sub>, salinity derived TA, temperature, and salinity

1 Fig. 1

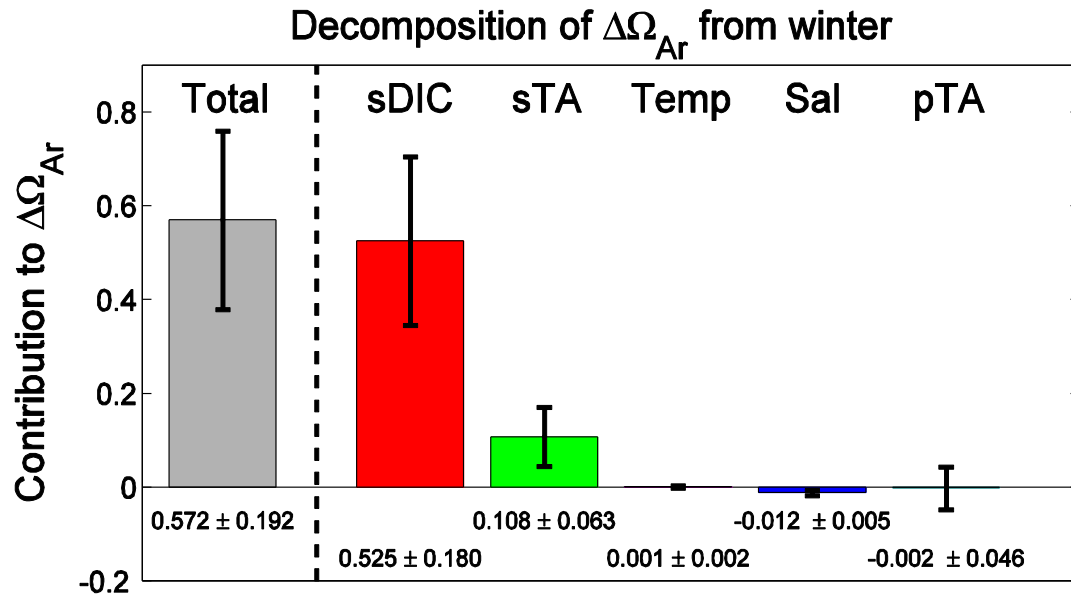


1 Fig. 2



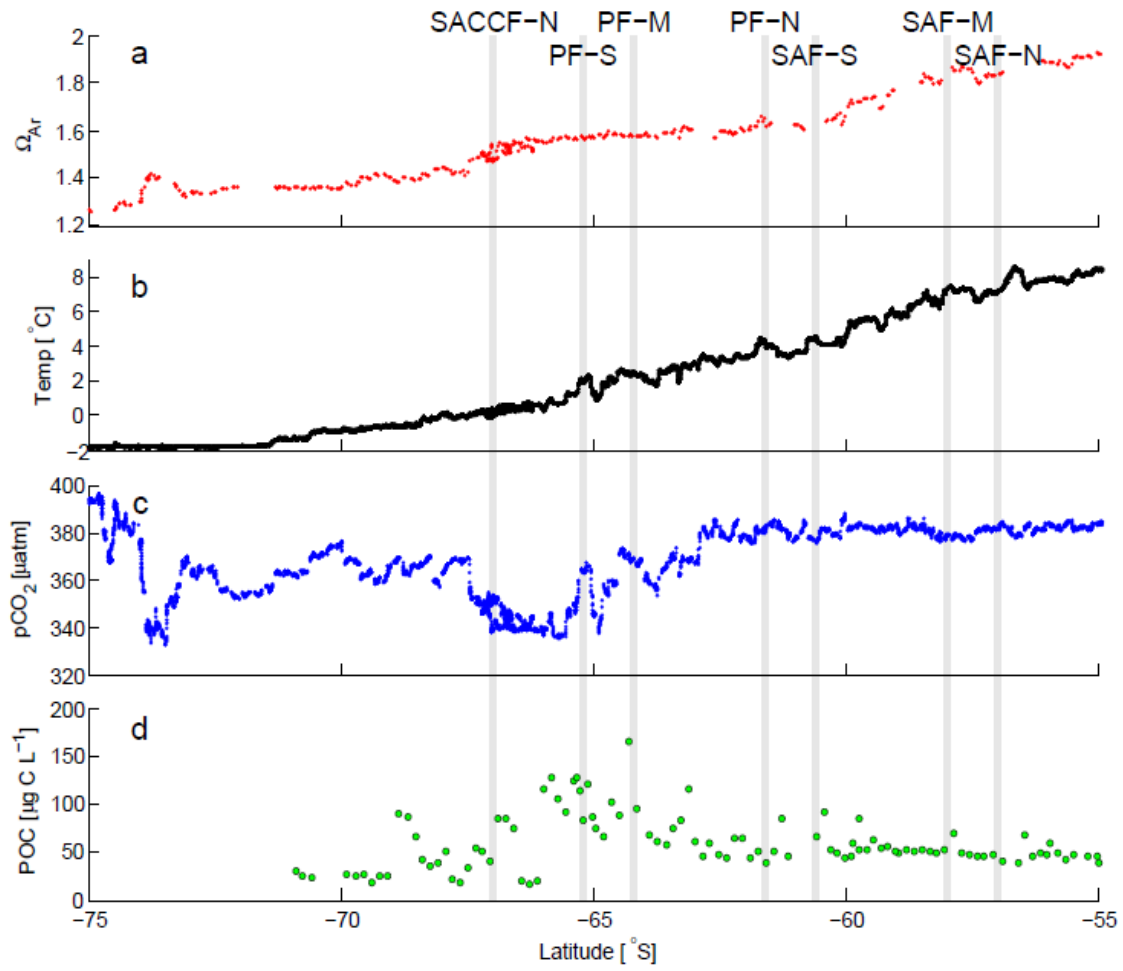
2

1 Fig. 3

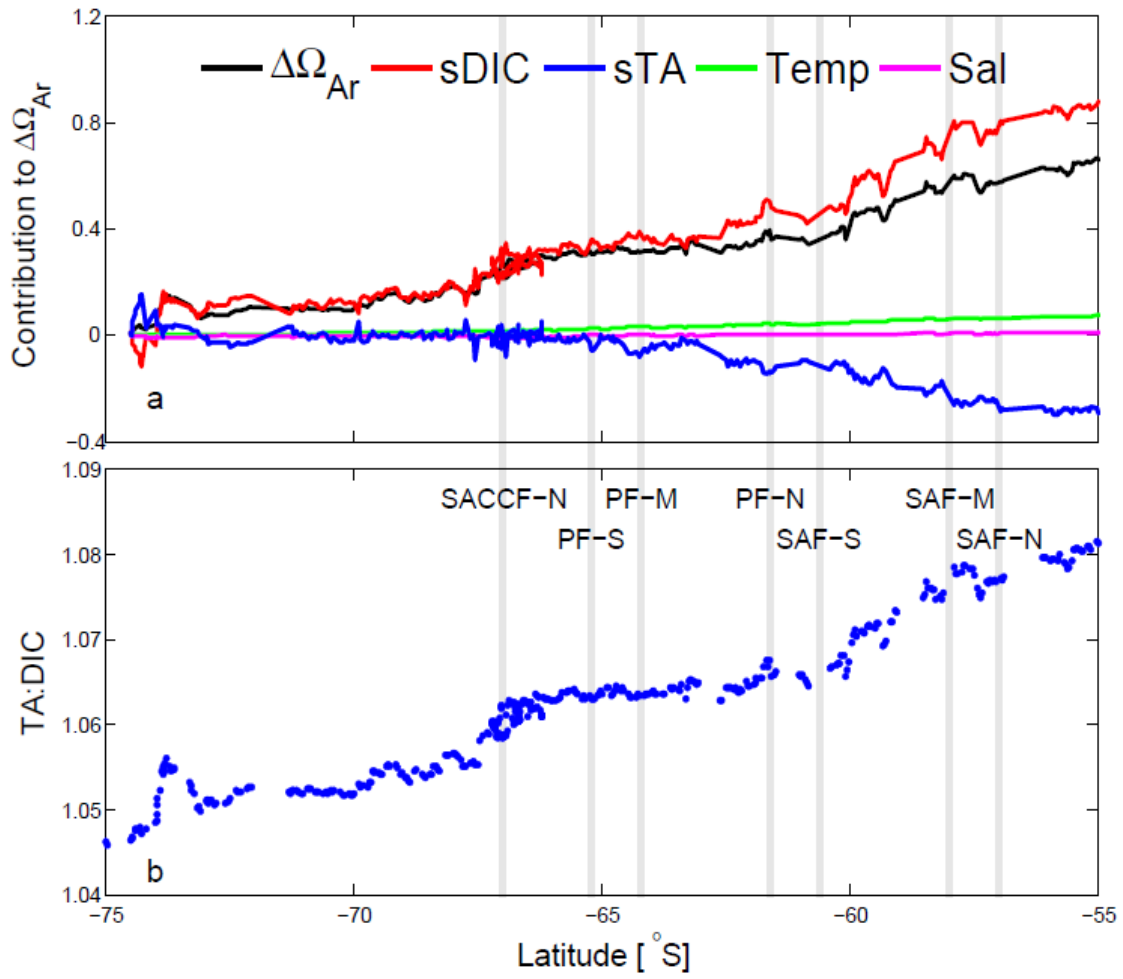


2

1 Fig. 4



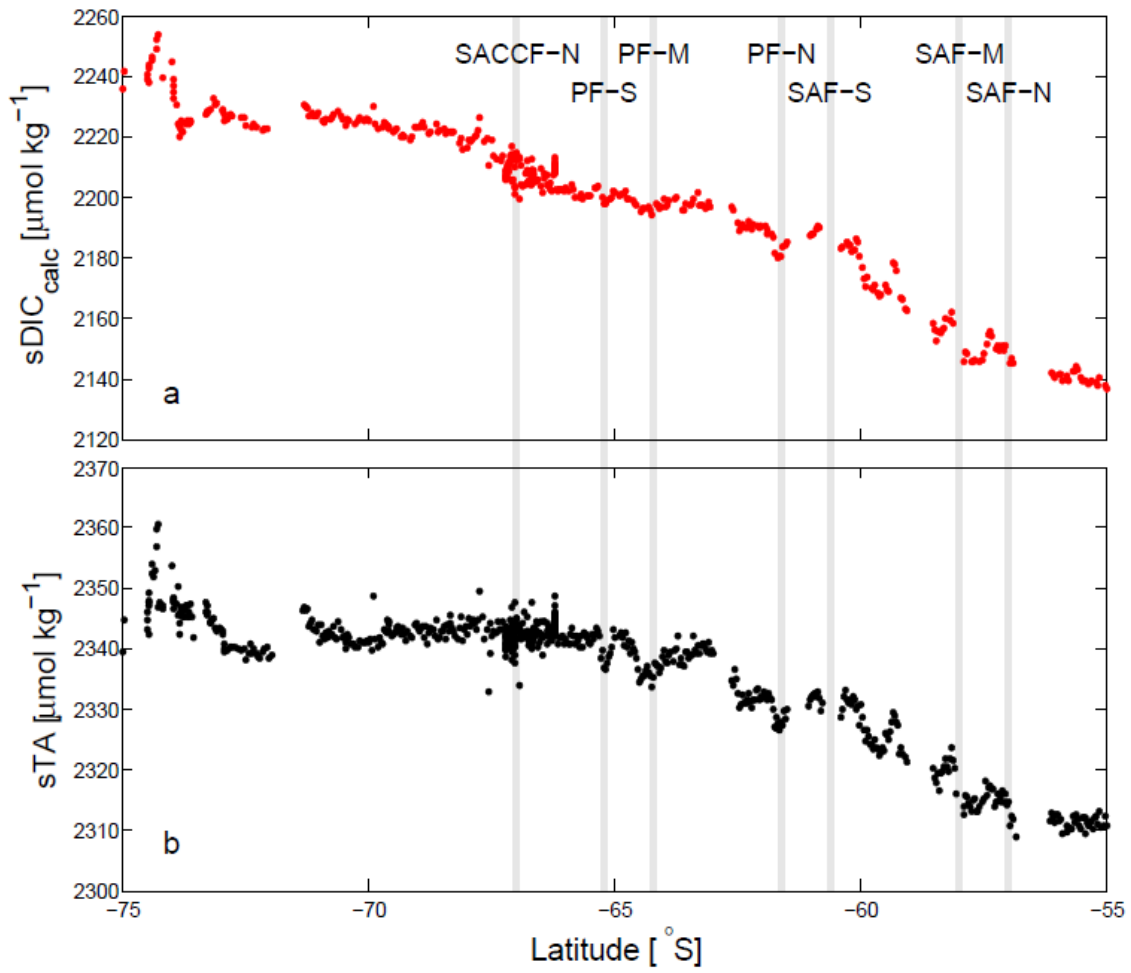
1 Fig. 5



2

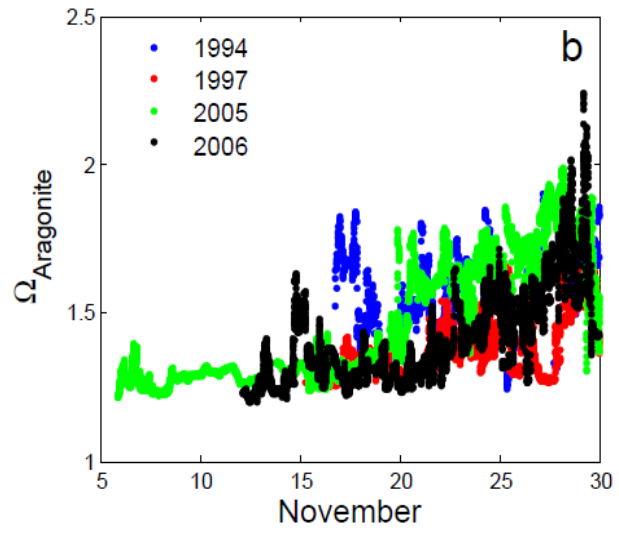
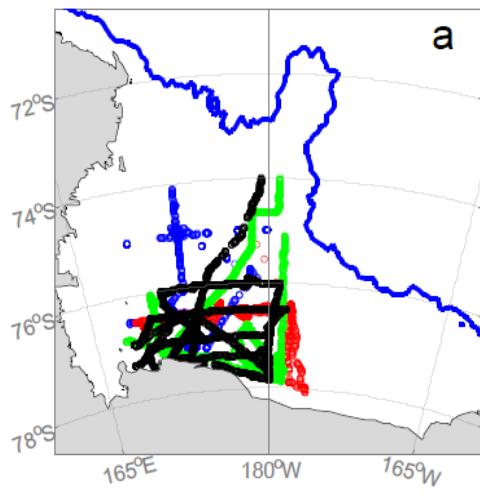


1 Fig. 6



2

1 Fig. 7



2

1 **Appendix**

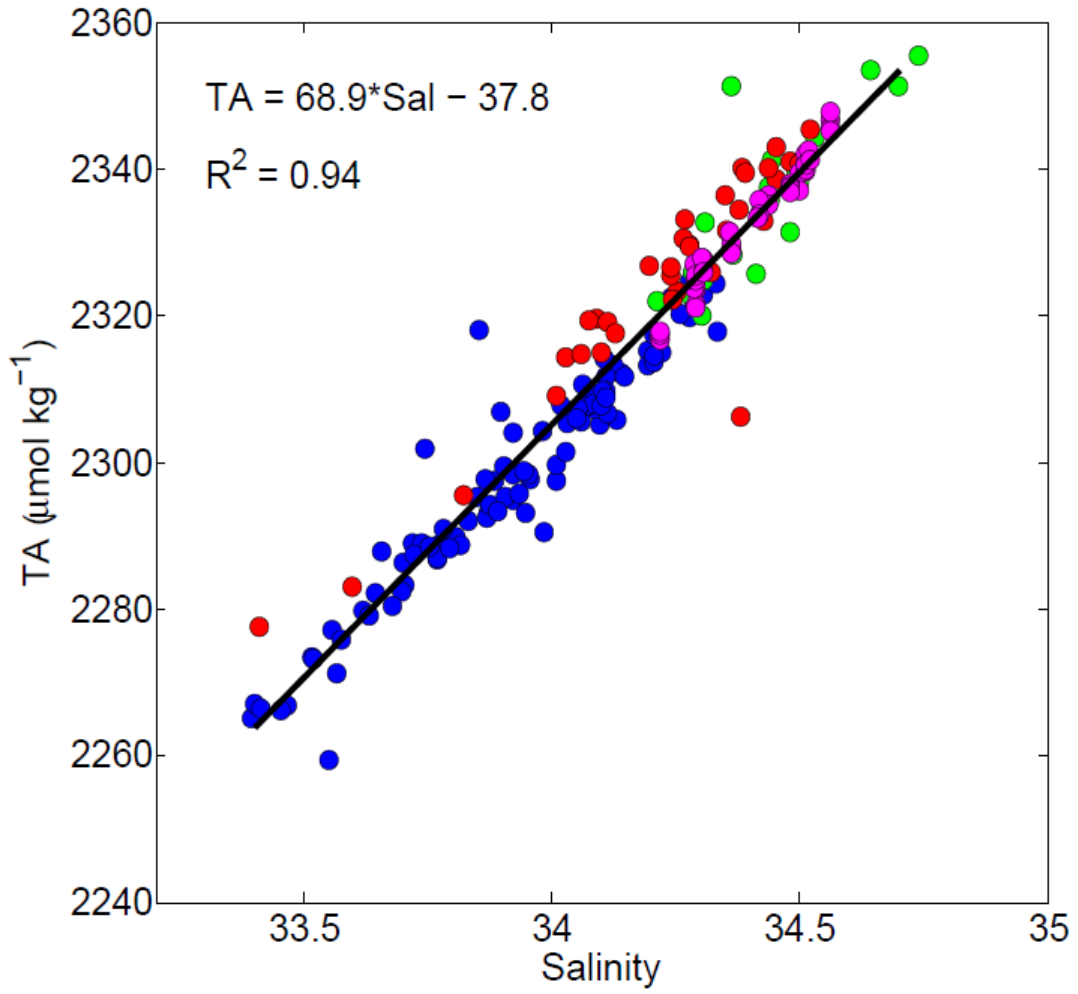
2

3 **Fig. A1.** Linear regression between TA and salinity with surface data from February – March  
4 2013 (blue, this study), November – December 1994 (green, Bates et al., 1998), December –  
5 January 1995/1996 (red, Bates et al., 1998), and April 1997 (magenta, Sweeney et al., 2000a).  
6 TA has been corrected to a nitrate concentration of  $29 \mu\text{mol kg}^{-1}$  to account for the effects of  
7 nitrate drawdown on TA (Brewer and Goldman, 1976).

8

9 **Fig. A2.** Profiles of aragonite saturation state ( $\Omega_{Ar}$ ) from off the Ross Shelf (see Fig. 2b) from  
10 the CLIVAR program (NBP 11-02) calculated from TA, DIC, temperature, and salinity at  
11 surface pressures.

1 Fig. A1



1 Fig. A2

